



# Exploratory study of the EU-DEMO Water-Cooled Lithium Lead breeding blanket behaviour in case of loss of cooling capability

G. Bongiovi<sup>a,\*</sup>, I. Moscato<sup>b</sup>, I. Catanzaro<sup>a</sup>, P.A. Di Maio<sup>a</sup>, E. Vallone<sup>a</sup>

<sup>a</sup> Università degli Studi di Palermo, Viale delle Scienze, Edificio 6, Palermo 90128, Italy

<sup>b</sup> Fusion Technology Department – Programme Management Unit, EUROfusion Consortium, Boltzmannstraße 2, Garching 85748, Germany

## ARTICLE INFO

### Keywords:

WCLL  
Breeding blanket  
Ex-vessel LOCA  
Transient analysis  
Decay heat

## ABSTRACT

Within the framework of the European Roadmap to the realization of fusion energy, a strong international cooperation is ongoing to develop a Breeding Blanket (BB) system for the EU-DEMO reactor. Although it is still to be decided whether the DEMO in-vessel components should perform any safety function, the pursuing of robust blanket concepts able to handle upset and accidental loading conditions has been always seen as good practice in fusion reactor engineering to enhance the inherent plant safety performances. Amongst the several classes of events that might challenge the BB structural integrity, the large Loss of Coolant Accident is one of the most relevant because it usually leads to a fast loss of cooling capability of the structures. Due to the characteristic of the tokamak assembly, the behaviour of each blanket segment during a sudden loss of cooling capability does not depend only upon distinguishing features of the component itself. In fact, the overall transient can be governed by conditions established in surrounding elements, like adjacent blanket segments and vacuum vessel, as well as by the plasma shutdown strategies adopted to protect the reactor.

The scope of the activity herein presented is to make a preliminary assessment of the intrinsic capability of EU-DEMO tokamak architecture to cope with the loss of cooling in the Water-Cooled Lithium Lead (WCLL) BB concept. Evaluation of BB thermal field in short and medium term under simplified, yet conservative, assumptions was carried out for four transient scenarios with the aim of investigating the response of the structure in case of: a) fast or soft plasma shutdown, and b) different blanket cooling schemes. Moreover, the WCLL BB thermo-mechanical response in the most critical time steps has been assessed. The obtained results shall help for future decisions on safety systems/action to be implemented to cope with accidents.

## 1. Introduction

The European Roadmap to the realization of fusion energy [1] establishes that DEMO will be the first fusion reactor able to produce hundreds of MWs of net electric power. To this goal, the EUROfusion consortium is running an ambitious research programme aimed at the selection of the most appropriate and efficient technology solutions. In this regard, the design of the DEMO breeding blanket (BB) and of its primary heat transfer system (PHTS) is definitely a key aspect, since the combined action of the two systems allow the heat power generated by the fusion reactions being recovered and converted, downstream several steps, to the electric power.

Although it is still to be decided whether the DEMO in-vessel components, like the BB, should perform any safety function, the pursuing of robust BB concepts able to handle upset and accidental loading

conditions has been always seen as good practice in fusion reactor engineering to enhance the inherent plant safety performances. Amongst the several classes of events to be considered in the BB structural design, the large Loss of Coolant Accident (large LOCA) is one of the most relevant because it usually leads to a fast loss of cooling capability of the structures. Hence, the occurrence of such a kind of event may jeopardise the BB system structural integrity because of the high temperatures achieved. In this regard, it has to be observed that the behaviour of each blanket segment during a sudden loss of cooling capability does not depend only upon the component itself, since the overall transient strongly depends on the conditions of the surrounding environment. In fact, adjacent blanket segments and vacuum vessel, as well as the plasma termination mode adopted to protect the reactor once the accident occurrence has been detected, play a significant role in the determination of the transient evolution. Therefore, a global evaluation is

\* Corresponding author.

E-mail address: [gaetano.bongiovi@unipa.it](mailto:gaetano.bongiovi@unipa.it) (G. Bongiovi).

<https://doi.org/10.1016/j.fusengdes.2023.113706>

Received 7 September 2022; Received in revised form 17 March 2023; Accepted 25 March 2023

Available online 29 March 2023

0920-3796/© 2023 The Authors. Published by Elsevier B.V. This is an open access article under the CC BY license (<http://creativecommons.org/licenses/by/4.0/>).

**Table 1**  
Summary of the assessed load cases.

	Soft plasma termination (plasma landing w/o disruption)	Fast plasma termination (plasma landing w disruption)
<b>Case A</b>	<b>Adiabatic SWs</b>	<b>Adiabatic SWs</b>
	<ul style="list-style-type: none"> <li>• 0 s: accident occurrence</li> <li>• 0–3 s: mass flow rate decreasing, plasma at full power</li> <li>• 3–123 s: fusion power ramp-down</li> <li>• 123 s - ∞: decay heat only</li> </ul>	<ul style="list-style-type: none"> <li>• 0 s: accident occurrence</li> <li>• 0–3 s: mass flow rate decreasing, plasma at full power</li> <li>• 3 s: plasma shut-down</li> <li>• 3 s - ∞: decay heat only</li> </ul>
<b>Case B</b>	<b>Diabatic SWs</b>	<b>Diabatic SWs</b>
	<ul style="list-style-type: none"> <li>• 0 s: accident occurrence</li> <li>• 0–3 s: mass flow rate decreasing, plasma at full power</li> <li>• 3–123 s: fusion power ramp-down</li> <li>• 123 s - ∞: decay heat only</li> </ul>	<ul style="list-style-type: none"> <li>• 0 s: accident occurrence</li> <li>• 0–3 s: mass flow rate decreasing, plasma at full power</li> <li>• 3 s: plasma shut-down</li> <li>• 3 s - ∞: decay heat only</li> </ul>

necessary to investigate the thermal and thermo-mechanical performances of the DEMO BB under the sudden Loss of Coolant conditions.

To this goal, the exploratory study of the EU-DEMO Water-Cooled Lithium Lead (WCLL) BB thermo-mechanical behaviour in case of loss of cooling capability has been performed at the University of Palermo, in close cooperation with the DEMO Central Team. In particular, transient thermal and thermo-mechanical analysis has been performed focussing on the equatorial region of the WCLL Central Outboard Blanket (COB) segment. Starting from the nominal steady state loading conditions (i.e. the end of flat top plasma state), the sudden loss of coolant has been postulated and the time-dependant thermal behaviour of the WCLL COB segment's equatorial region has been firstly investigated. To this purpose, different plasma termination modes (fast and soft) and different cooling schemes for the surrounding BB segments (direct and alternate cooling, corresponding to the total or partial loss of cooling capability in the whole BB system) have been assumed, so to assess four different transient load cases. Secondly, the corresponding thermo-mechanical transient analysis has been performed in order to investigate the structural response of the component over the time, in view of the RCC-MRx structural design code [2].

The scope of the work has been the preliminary investigation of the WCLL BB capabilities of removing the deposited thermal power by thermal radiation towards the surrounding components (vacuum vessel and adjacent blanket segments) and of fulfilling the prescribed structural design criteria, once the cooling in the BB system is totally or partially lost. In particular, the study has been mainly aimed at evaluating the inherent capability of WCLL BB structures to withstand soft plasma shutdown, investigating its thermal and thermo-mechanical behaviour in short, medium and long term under simplified (yet conservative) assumptions. The study has been performed adopting a theoretical-numerical approach based on the Finite Element Method (FEM) by means of the commercial Abaqus FEM code. The obtained results, herewith presented and critically discussed, shall help for future decisions on safety systems/action to be implemented to cope with accidents.

## 2. The adopted methodology

The scope of the reported activity has been the assessment of the transient thermal and thermo-mechanical behaviour of the WCLL BB in case of a sudden loss of coolant, deriving for instance from a large loss of coolant accident. To this end, un-coupled transient thermal and thermo-mechanical analyses have been carried out.

From the thermal point of view, a multi-step transient analysis has been performed. First, a steady state step has been launched in order to carry out the steady state thermal field under the nominal WCLL BB

loading conditions, corresponding to the loading conditions characterising the end of flat-top plasma state. Then, the occurrence of the loss of coolant capability has been postulated and the transient step has begun. In particular, an accident detection time of 3 s has been assumed, considering that in this timespan the coolant mass flow linearly decreases to zero due to the accident while the plasma is still in a full-power mode since the accident has not been detected yet. Then, two different plasma termination modes have been alternately considered. From one hand, the fast plasma termination mode has been imposed, assuming that once the accident is detected the plasma is immediately terminated with a disruption. From the other hand, the soft plasma termination mode has been assessed, assuming that once the accident is detected the plasma is terminated without disruption, following a ramp-down lasting for 120 s. During the plasma ramp-down, the power (both in terms of deposited nuclear power and heat flux impinging onto the First Wall) has been considered decreasing following the ramp. In both the cases, after the plasma termination, the unique heat power source is represented by the decay heat power, whereas the radiation toward the Vacuum Vessel (VV) has been kept as heat sink. Hence, the capabilities of the WCLL BB to remove the deposited thermal power by irradiation towards the VV once the cooling is totally lost has been evaluated. Such a condition corresponds to a uniform BB system cooling strategy, which implies the total loss of cooling capability in case of accident. In addition, a scenario foreseeing the Side-Walls (SWs) able of radiating towards the adjacent BB segments (then supposing the BB segments actively cooled following an alternate scheme so to lose, in case of accident, the cooling only in a half of the whole BB system) has been investigated too, in both the plasma termination modes. In this way, the impact of different BB system cooling schemes on the heat removal capabilities in case of the sudden loss of coolant in an adjacent segment is studied as well. Therefore, in total, four load cases (summarized in the following Table 1) have been defined and assessed.

From the mechanical point of view, the corresponding thermo-mechanical analyses have been performed. In particular, each analysis consists in a series of static steps, each considering the thermal field calculated at a certain time of the thermal transient and the corresponding pressure load, assuming as reference condition the deformative state calculated at the end of the previous static step. In this way, it has been possible evaluating the evolution of the ratios between the stress intensities and the stress limits characterising the set of criteria prescribed by the RCC-MRx structural design code, along purposely selected paths. Due to the accidental nature of the loading scenarios, they have been considered as Level D events.

## 3. The wcll BB COB segment

In the study here reported, the v0.6b version of the WCLL COB geometric layout has been considered [3]. In particular, the attention has been paid to the COB segment's equatorial region, as shown in Fig. 1. Its layout includes two adjacent radial-toroidal cells, poloidally delimited by two half horizontal Stiffening Plates (horizontal SPs). As per the reference configuration [3], each radial-toroidal cell is equipped with a bundle of 22 Double-Walled Tubes (DWTS) and its Segment Box (SB), namely the First-Wall (FW) plus SWs complex, is endowed with 4 radial-toroidal cooling channels. Thus, the considered geometric model encompasses the proper portion of the SB, of the horizontal and vertical SPs, of the baffle plates, of the Back-Supporting Structure (BSS), of the Back-Plates (BPLs) plus the Manifolds as well as of the W layer covering the SB (in orange in Fig. 1). In addition, the PbLi breeder has been included in the model too (in yellow in Fig. 1), as well as the cooling water (in pale blue in Fig. 1) flowing throughout the SB channels and the DWTS, allowing a more detailed assessment of the WCLL COB equatorial region thermal behaviour. Moreover, Eurofer steel has been considered as structural material. The temperature-dependant thermo-physical properties of such materials, drawn from [4–6], have been considered for the study and reported, for the sake of completeness, in the following

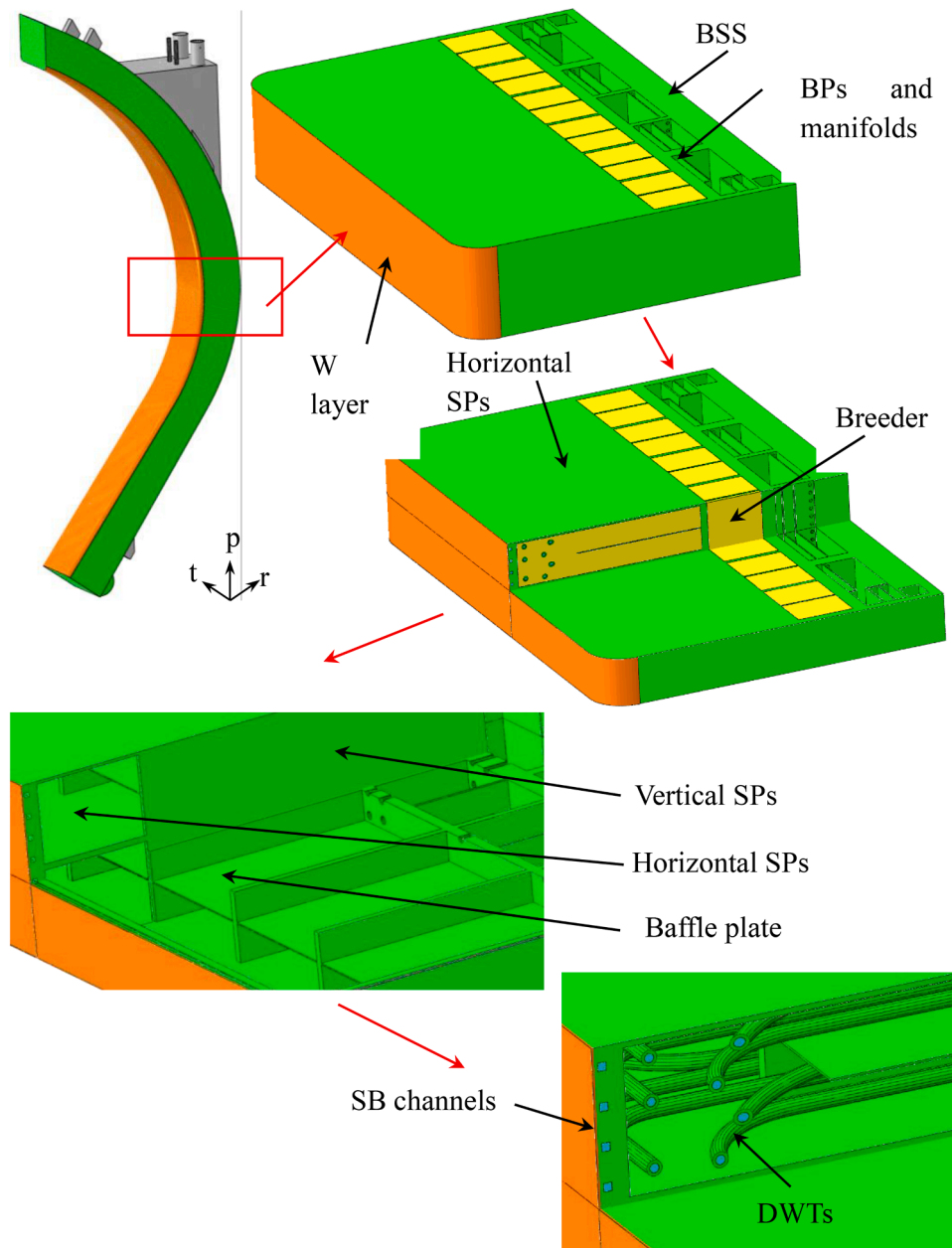


Fig. 1. The geometric model of the WCLL COB segment's equatorial region in the v0.6b layout.

**Table 2**  
Eurofer thermo-physical properties [4].

T [°C]	$\rho$ [kg/m <sup>3</sup> ]	k [W/m•°C]	$c_p$ [J/kg•°C]	$\alpha$ [10 <sup>-5</sup> /°C]	E [GPa]	$\nu$
20	7744	28.1	449.2	1.03	217	0.3
50	7750	28.9	-	1.05	215	
100	7740	29.8	490.0	1.07	212	
200	7723	30.4	520.2	1.12	207	
300	7691	30.0	545.8	1.16	202	
400	7657	29.5	587.0	1.19	196	
500	7625	29.6	663.6	1.22	190	
600	7592	31.1	795.7	-	170	
700	7559	-	1003.4	-	162	

**Table 3**  
Pb-15.7Li thermo-physical properties [5].

T [°C]	$\rho$ [kg/m <sup>3</sup> ]	k [W/m•°C]	$c_p$ [J/kg•°C]
20	10,172	7.69	192
300	9839	13.18	190
350	9779	14.16	189
400	9720	15.14	189
450	9661	16.12	188
500	9601	17.10	188
550	9542	18.08	187
600	9482	19.06	187
650	9423	20.04	187
700	9363	21.02	186

**Table 4**  
Tungsten thermo-physical properties [6].

T [°C]	$\rho$ [kg/m <sup>3</sup> ]	k [W/m•°C]	$c_p$ [J/kg•°C]	$\alpha$ [10 <sup>-6</sup> /°C]	E [GPa]	$\nu$
20	19,300	162.7	138.9	4.40	396.1	0.280
100		156.4	139.7	4.41	396.0	0.281
200		149.4	140.8	4.42	393.8	0.281
300		143.2	142.0	4.44	391.9	0.282
400		137.7	143.3	4.46	389.3	0.283
500		133.0	144.7	4.49	386.3	0.284
600		128.8	146.2	4.52	382.7	0.285
700		125.0	147.8	4.56	378.5	0.287

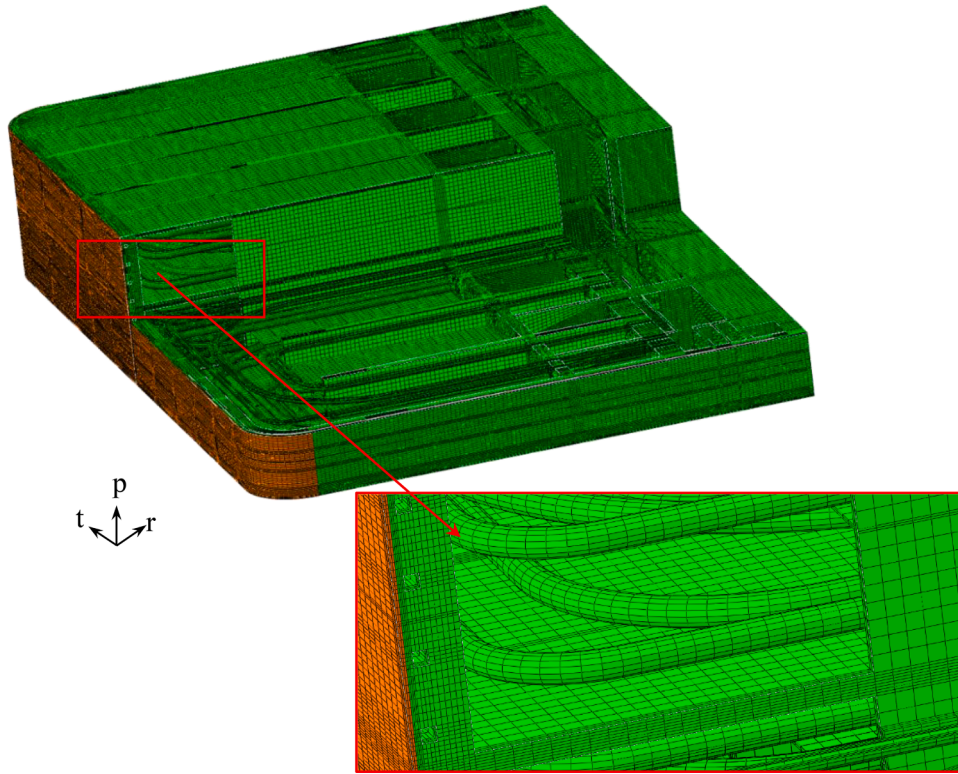


Fig. 2. Views of the mesh set-up.

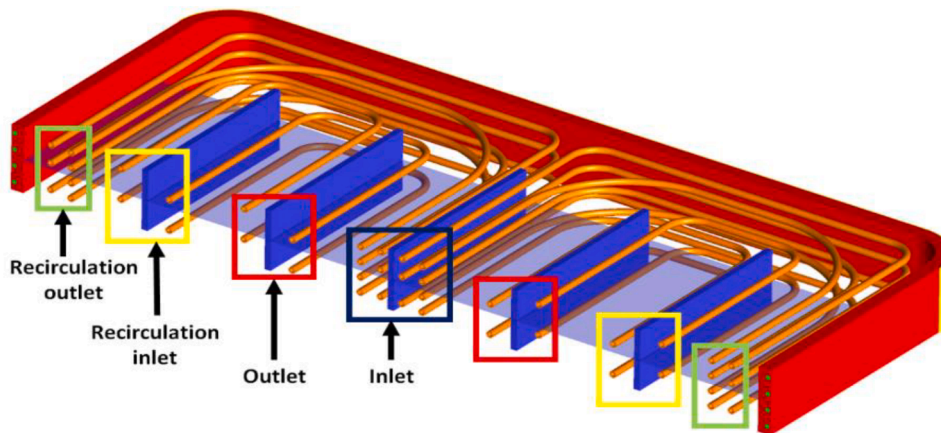


Fig. 3. The DWTs layout and the recirculation scheme [3].



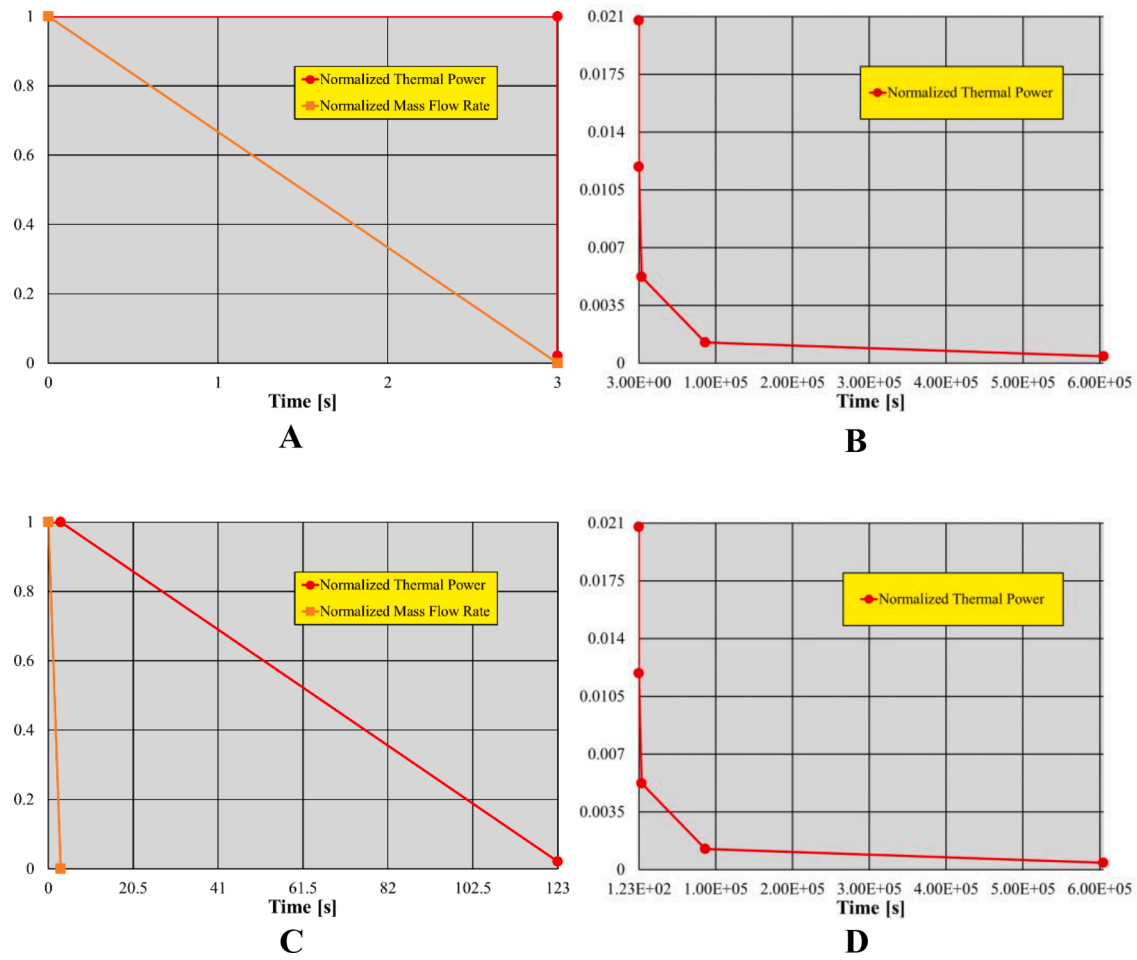


Fig. 4. Normalized thermal power and mass flow rate in case of fast (A and B) and soft (C and D) plasma termination mode.

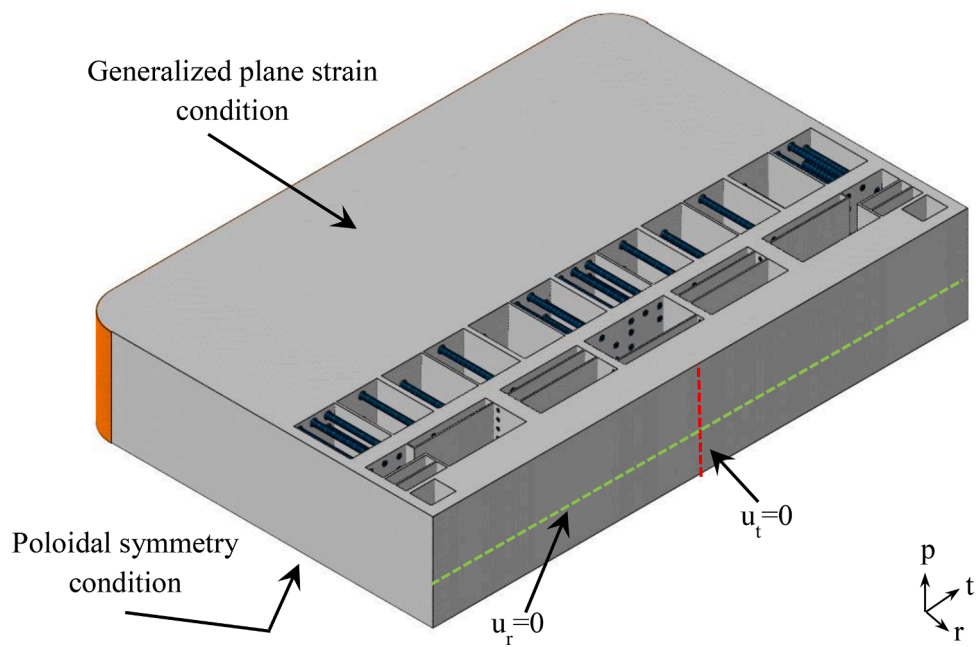


Fig. 5. The set of mechanical restraints.

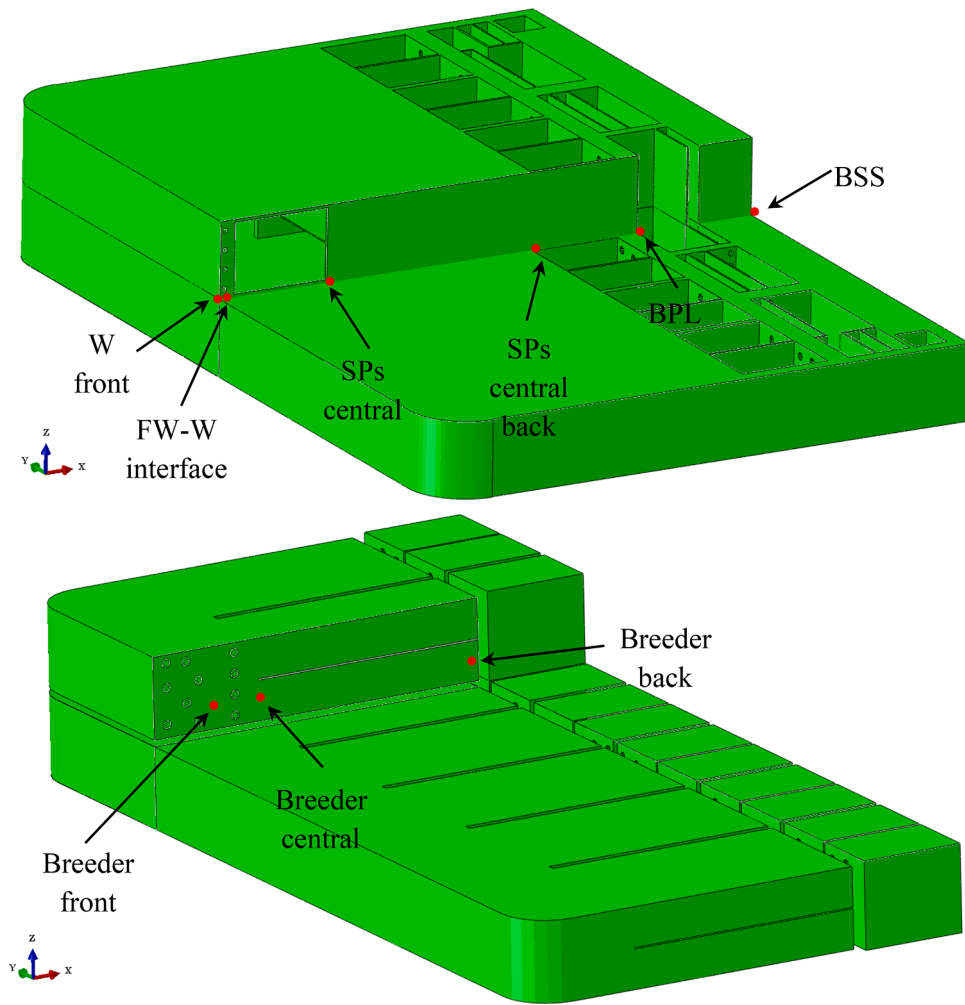


Fig. 6. The selected control nodes for the temperature trends evaluation.

**Table 5**  
Thermal balance in the steady-state conditions.

Deposited Power	Radiative Power	Total Provided Power	Total Removed Power
470 kW	109.6 kW	579.6 kW	559.4 kW

Tables 2–4.

#### 4. The FEM model

In order to perform the transient thermal and thermo-mechanical analysis of the WCLL COB segment's equatorial region in the four load cases selected, proper 3D FEM models have been developed changing the loads and boundary conditions coherently with the considered load case.

Starting from the geometric configuration described in the previous section, a mesh consisting of  $\sim 5.6$  M nodes connected in  $\sim 13.0$  M tetrahedral and hexahedral elements has been set-up. The adopted mesh settings ensure the best compromise in between results accuracy and saving of computational burden, since they derive from past campaigns of thermo-mechanical analysis of the WCLL BB in which mesh independence assessments were carried out [7,8]. As it can be observed in Fig. 2, the SB and the SPs have been discretized with a large number of elements, to ensure a good accuracy of results especially in the stress linearization procedure.

#### 4.1. Thermal loads and boundary conditions

As far as thermal loads and boundary conditions are concerned, in the first step of the analysis the DEMO WCLL BB steady state nominal conditions have been assumed in order to predict the steady state thermal field. Hence, the following loads and boundary conditions have been assumed:

- heat flux acting onto W plasma facing surface (orange component in Fig. 1) equal to  $0.27 \text{ MW/m}^2$  [9] on the FW straight region and decreasing to 0 according to a cosine law onto the SW bending surfaces;
- 3D spatial distribution of the nuclear deposited heat power density within Eurofer (green domain in Fig. 1), breeder (yellow domain in Fig. 1) and tungsten [10];
- 3D spatial distribution of the decay heat power density within Eurofer domain [11];
- forced convective heat transfer within both SB cooling channels (Fig. 1) and DWTs. To this purpose, the water recirculation in between the DWTs has been simulated [3] (Fig. 3) and the counter-current flow has been assumed for the SB channels. In order to investigate more realistically the heat transfer between the cooling water and the channels/tubes surfaces, the so-called “frozen” flow field FEM approach has been adopted. This means that a bulk temperature equal to  $295 \text{ }^\circ\text{C}$  has been assigned to the water entering the SB channels and the DWTs together with a purposely calculated value of the convective Heat Transfer Coefficient (HTC). In this way,

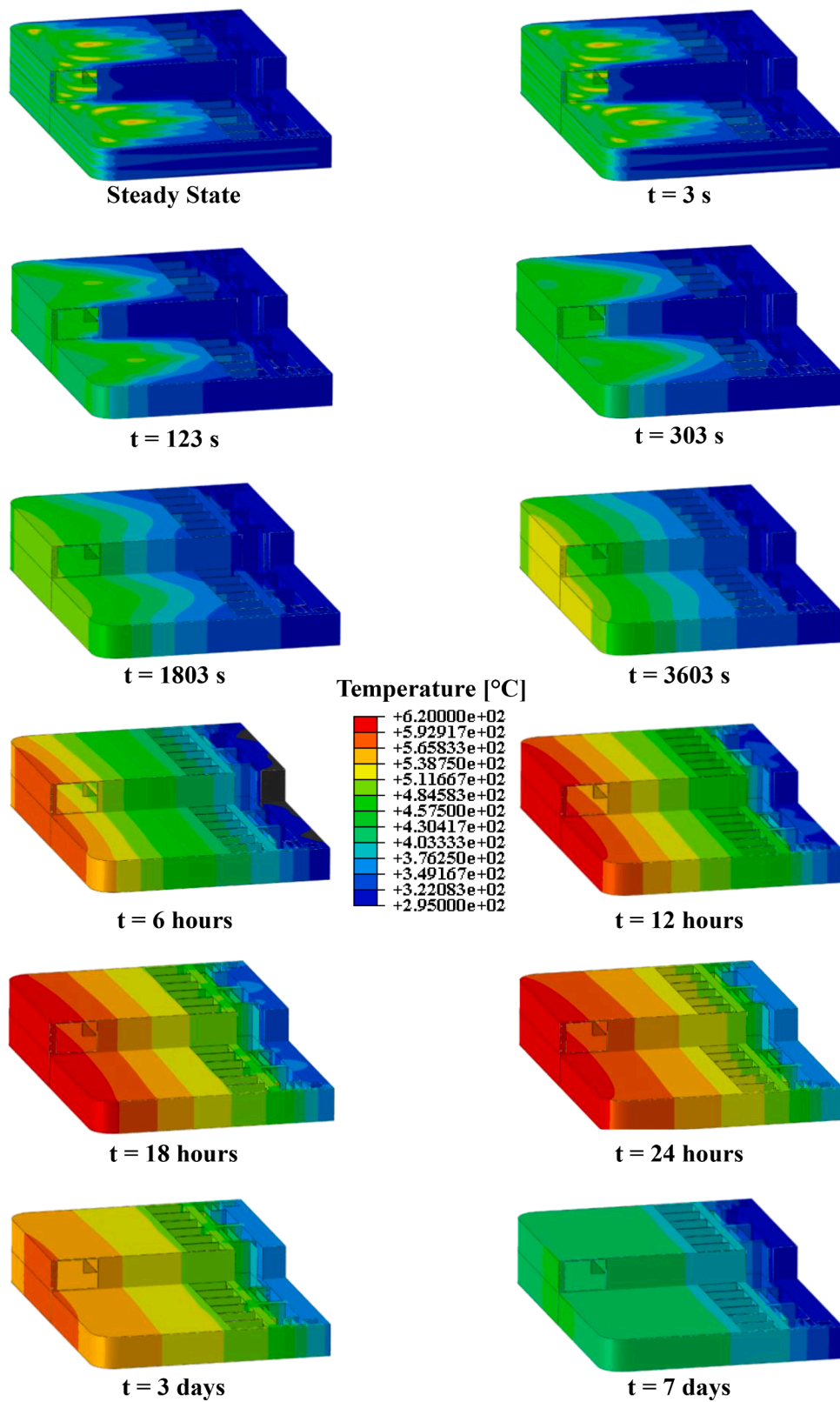


Fig. 7. Eurofer thermal field over the time – Fast plasma termination mode “Case A”.

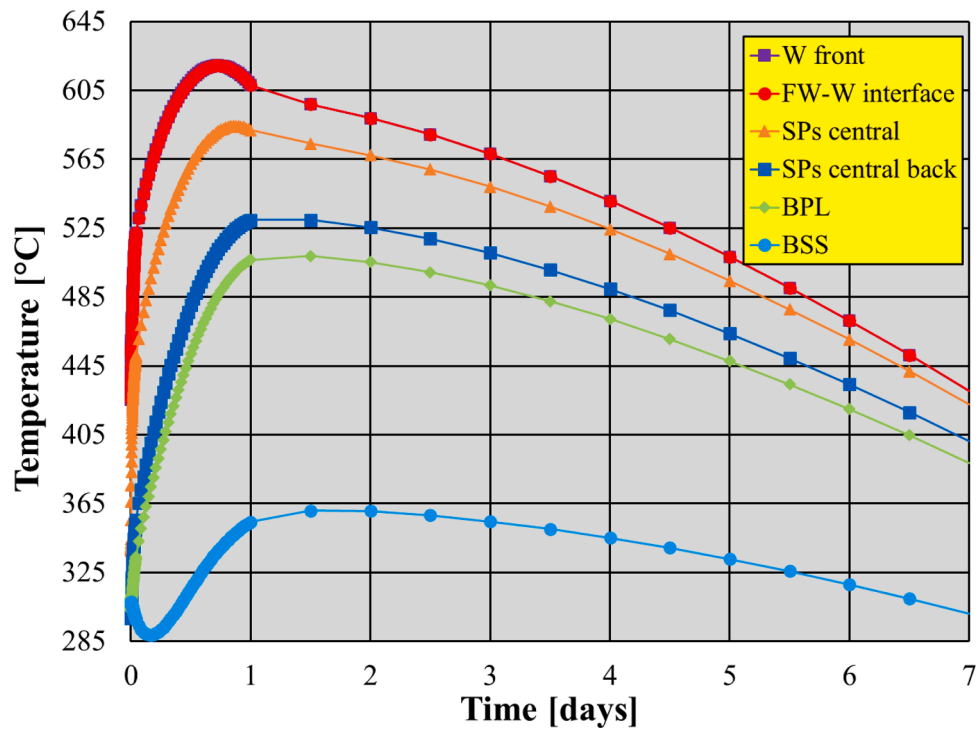


Fig. 8. Eurofer temperature trends at the control nodes - Fast plasma termination mode “Case A”.

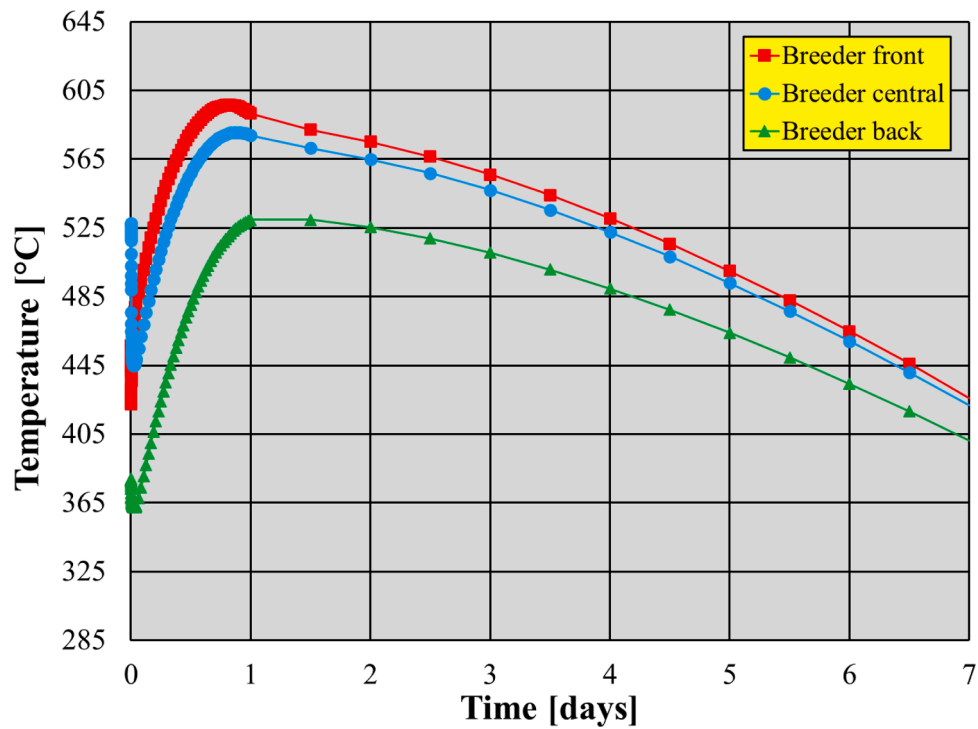


Fig. 9. Breeder temperature trends at the control nodes - Fast plasma termination mode “Case A”.



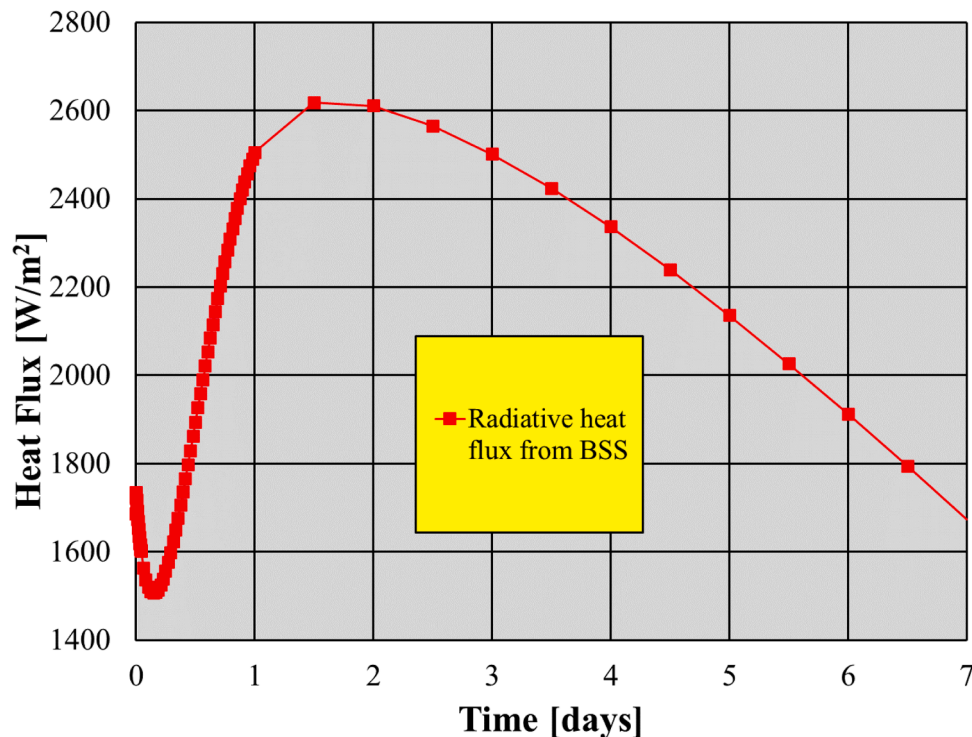


Fig. 10. Heat flux radiated from the BSS - Fast plasma termination mode “Case A”.

it is possible to calculate the bulk temperature evolution along each channel/tube abscissa, modelling the convective heat transfer with an increased level of detail. The steady state analysis has been iterated so to obtain HTC values able of ensuring the design thermal rise of 33 °C [3] between inlet and outlet of each SB channel and DWT. In particular, a HTC value of 34,541 W/(m<sup>2</sup> °C) has been found for the SB channels, whereas HTC of 17,107 W/(m<sup>2</sup> °C) and of 26,767 W/(m<sup>2</sup> °C) have been assumed for the 1st and for the 2nd round of DWTs, respectively;

- thermal radiation from the BSS (Fig. 1) toward the VV at 60 °C with emissivity equal to 0.3. Since the VV totally surrounds the BB, in order to simplify the model the thermal radiation has been supposed happening towards the environment assumed at the VV temperature;
- thermal coupling between the top and bottom radial-toroidal faces of the model;
- perfect thermal contact in between steel and breeder, the latter considered as still.

Afterwards, the transient behaviour in case of sudden loss of coolant has been investigated in the four selected load cases. In case of fast plasma termination mode, the trends of the normalized deposited thermal power and of the normalized coolant mass flow rate are reported in Fig. 4. As it can be observed in Fig. 4A, in the time span 0–3 s the mass flow rate decreasing to 0 due to the accident whereas the plasma is still at full power due to the delay in the reaction. At  $t = 3$  s, the accident is detected and the plasma is immediately terminated. This means that no heat flux nor neutronic power acts on the BB anymore. From this point on, only the time-dependant spatial distribution of decay heat power is assumed as thermal load (Fig. 4B), according to the data reported in [11]. Hence, the pure diffusive heat transfer mode within the BB structure and breeder is assumed, as well as the radiation from BSS toward VV at 60 °C with emissivity equal to 0.3. As specified in Table 1, this is the “Case A” scenario, and corresponds to a cooling strategy for the BB system foreseeing a uniform cooling which means the total loss of cooling in the BB system in case of accident. In addition, a fast plasma termination “Case B” has been assessed, in which the SWs have been

supposed able to radiate, throughout the transient, towards adjacent BB segment supposed at 311.5 °C with an emissivity value of 0.3. This corresponds to the assumption of an alternate cooling scheme for the BB segments, implying the loss of the cooling in only a half of the BB segments in case of accident whereas the other half is normally cooled remaining in steady state conditions.

In the same way, looking at Fig. 4, the trends of normalized deposited thermal power and mass flow rate in case of soft plasma shutdown can be observed. Here, after the detection time of 3 s, the fusion power ramp-down can be observed (Fig. 4C), linearly reducing the deposited thermal power from nominal value to ~ 2% of the BB nominal deposited power. In this case, also the plasma heat flux acting onto BB plasma facing surface has been assumed linearly decreasing according to the ramp. Then, after the shut-down (Fig. 4D), the same time-dependant decay heat power spatial distribution is assumed. Also for soft plasma termination mode analysis, both “Case A” and “Case B” cases have been investigated.

#### 4.2. Mechanical loads and boundary conditions

As to mechanical loads and boundary conditions, in the first step of the analysis the DEMO WCLL BB steady state nominal conditions have been assumed. Hence, the following loads and boundary conditions have been assumed:

- 3D thermal field calculated from the previous thermal analysis;
- design pressure onto the breeder and water wetted surfaces, calculated as the nominal pressure values multiplied by a safety factor of 1.15 [12]. Therefore, a pressure equal to 0.575 MPa has been imposed onto the breeder wetted surfaces, as well as a pressure load amounting to 17.825 MPa has been applied to the water wetted surfaces.
- a proper set of mechanical restraints in order to simulate the effect of the attachment system and of the not-simulated adjacent parts of the segment (Fig. 5). In particular, a generalized plane strain condition has been imposed to the nodes lying onto the upper boundary

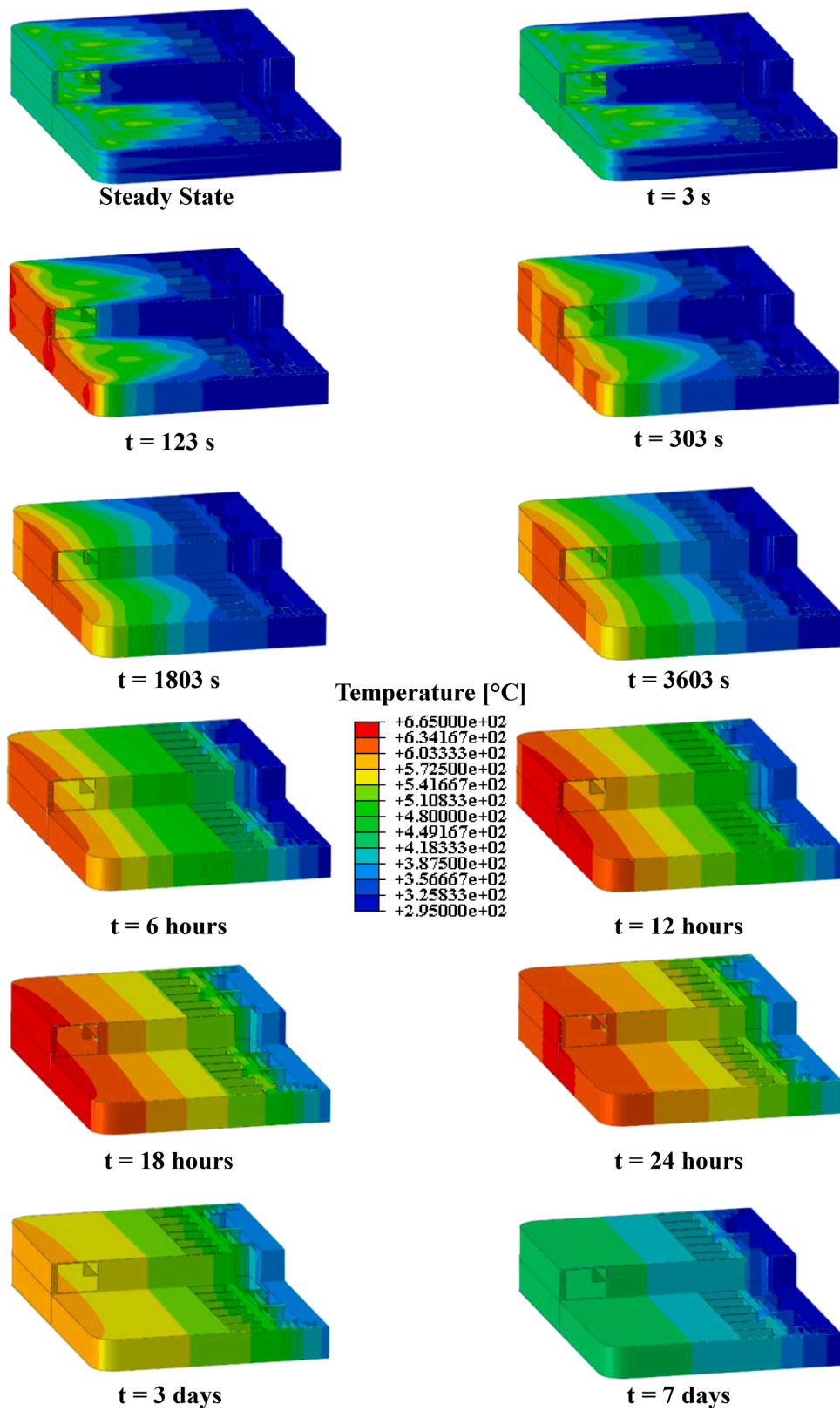


Fig. 11. Eurofer thermal field over the time – Soft plasma termination mode “Case A”.

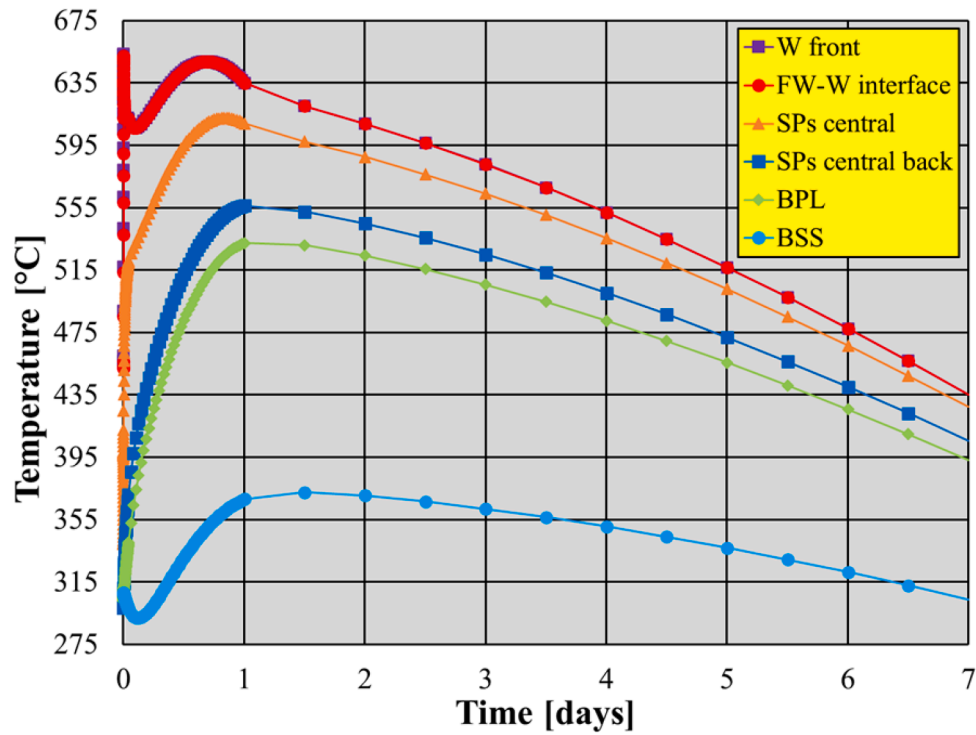


Fig. 12. Eurofer temperature trends at the control nodes - Soft plasma termination mode “Case A”.

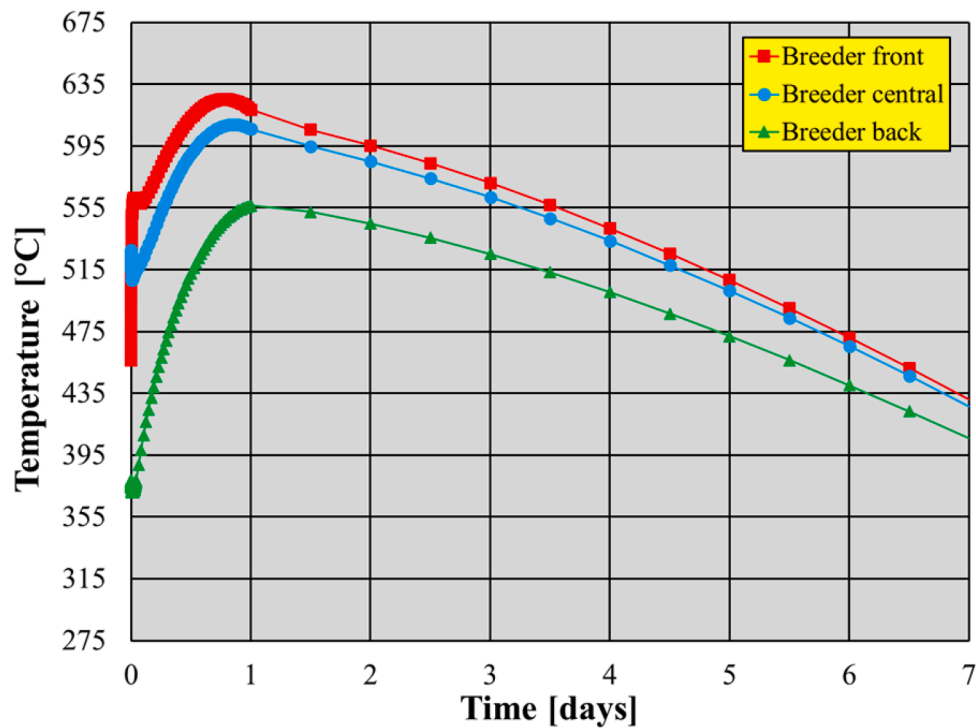


Fig. 13. Breeder temperature trends at the control nodes - Soft plasma termination mode “Case A”.

surface. The latter conditions means that the nodes of the interested surface are bounded to stay on a plane which is free to move poloidally and to tilt whit respect the radial and toroidal directions.

Afterwards, coherently with the assessed load case, the proper thermal field at each corresponding time step has been considered and the pressure onto the water wetted surfaces has been reduced to 0 in the

first 3 s after the accident occurrence.

### 5. Analysis and results

Adopting the FEM models described in the previous section, four different un-coupled thermal and thermo-mechanical transient analysis have been carried out under the four selected loading scenarios.

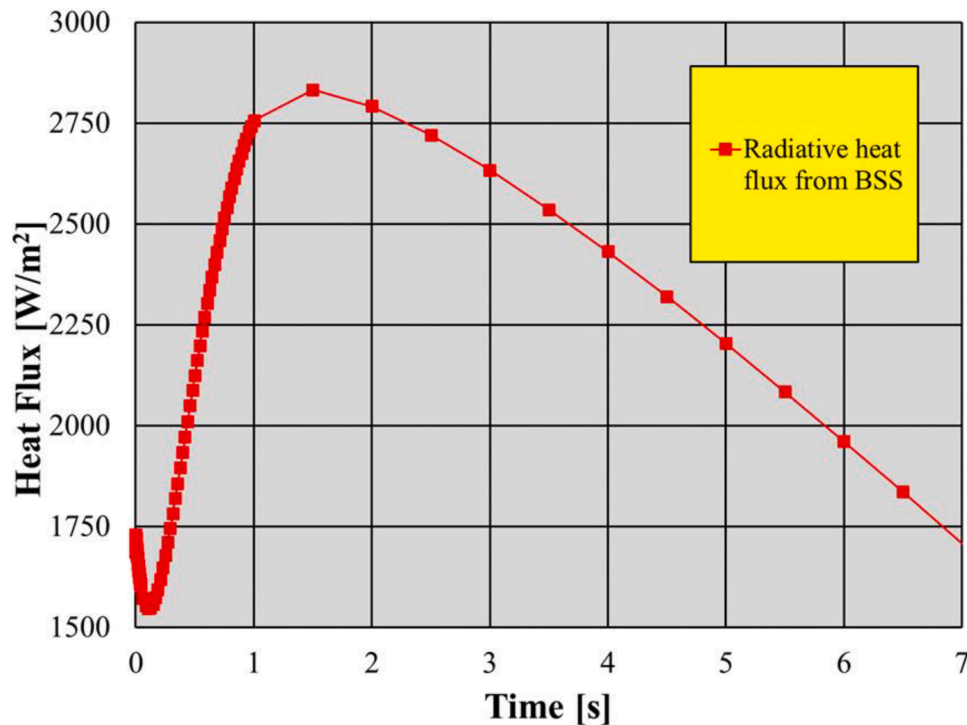


Fig. 14. Heat flux radiated from the BSS - Soft plasma termination mode “Case A”.

### 5.1. Thermal analysis results

The results obtained in terms of time-dependant thermal field and the evaluation of the thermal heat flux radiated over the time from the BSS and the SWs are reported in the following. In addition, the trends of the temperature at some control nodes belonging to the Eurofer and breeder domains are depicted for each scenario investigated (Fig. 6).

It has to be observed that the selected control nodes within Eurofer are located at different radial positions in correspondence of the intersection of the poloidal and toroidal symmetry planes of the model. Moreover, the control nodes belonging to the breeder domain are located at different radial positions in correspondence of the centre of the breeder pool with respect to the central vertical SP.

Since any transient analysis starts from the same steady-state condition, representative of the normal operation, the steady-state thermal balance at the end of the steady-state step is reported in Table 5.

Here, “Deposited Power” is the integral value of the volumetric nuclear heating. Since this output is not available in Abaqus, it has been estimated it as the sum of the products of the deposited power density ( $\text{W/m}^3$ ) value at the centroid of each element (available as output in Abaqus thanks to a proper workaround) multiplied by the volume of the corresponding element ( $\text{m}^3$ ). This estimation generates of course an inaccuracy, since the calculated value is not exactly equal to the value used by Abaqus code in its calculation even though it is the best way to estimate it. Instead, “Radiative Power” is the integral value of the surface heating, calculated by hand as it is not available as output too. The sum of these two calculated quantities is the “Total Provided Power”, whereas the “Total Removed Power” is the total power removed by the coolant, properly obtained as Abaqus output. As one can see, the difference in between the provided and the removed power is  $\sim 3\%$ . This is mainly attributable to the impossibility of obtaining as output the exact amount of the volumetric heating integral value, which is therefore estimated.

#### 5.1.1. Fast plasma termination “Case A”

The Eurofer thermal field over the time predicted under the fast plasma termination “Case A” scenario is shown in Fig. 7. As it can be

observed, even if the plasma is immediately terminated, starting from steady state values the temperature increases significantly in the first 24 h after the accident, widely exceeding the suggested limit value of  $550\text{ }^\circ\text{C}$  within FW and breeding zone steel for a quite long timespan. Even after 3 days, the Eurofer temperature is well above the  $500\text{ }^\circ\text{C}$ . After 7 days, temperatures ranging from  $\sim 400\text{ }^\circ\text{C}$  to  $\sim 445\text{ }^\circ\text{C}$  are still predicted, suggesting that an auxiliary system should be conceived to speed-up the BB cooling in such a scenario. It has to be also noted that in the first 3 s after the accident occurrence, when the coolant mass flow goes to zero whereas the plasma is still at full power, no significant temperature variations are predicted. This is due to the high thermal inertia of the BB system. Moreover, the temperature trends versus time obtained at the control nodes for Eurofer and breeder are reported in Figs. 8 and 9, respectively. As it can be observed, at the FW-W interface, a maximum temperature of  $619.5\text{ }^\circ\text{C}$  is achieved  $\sim 17.5$  h after the accident. Concerning the breeder domain, it can be noted that the maximum temperature of  $596.6\text{ }^\circ\text{C}$  is achieved after  $\sim 19.5$  h in the control node “breeder front”.

In the end, in Fig. 10, the trend of the heat flux radiated from the BSS is shown. As it can be observed, after an initial decrease (the minimum heat flux of  $\sim 1500\text{ W/m}^2$  is radiated after 3.5 h) the radiative heat flux power grows up to its maximum value of  $\sim 2600\text{ W/m}^2$ , achieved after 1.5 days from the accident which is also when the temperature predicted in the BSS control node achieves its maximum value ( $\sim 361\text{ }^\circ\text{C}$ ). Then, the radiated heat flux starts to decrease again. Assuming for the whole BB system a BSS total surface of  $1650\text{ m}^2$  (in this case a direct BB cooling scheme is assumed, hence the accident occurrence implies the total loss of cooling) it can be estimated that the thermal power radiated toward the VV ranges from  $\sim 2.5$  to  $\sim 4.3$  MW. This last information can help in the design of the VV cooling system.

#### 5.1.2. Soft plasma termination “Case A”

As it can be observed from the Eurofer thermal field (Fig. 11), the soft shutdown causes high temperatures within the FW in the first 120 s after the accident detection, i. e. during the plasma ramp-down. Moreover, starting from steady state values the temperatures increase significantly in the first 24 h after the accident occurrence, widely exceeding the



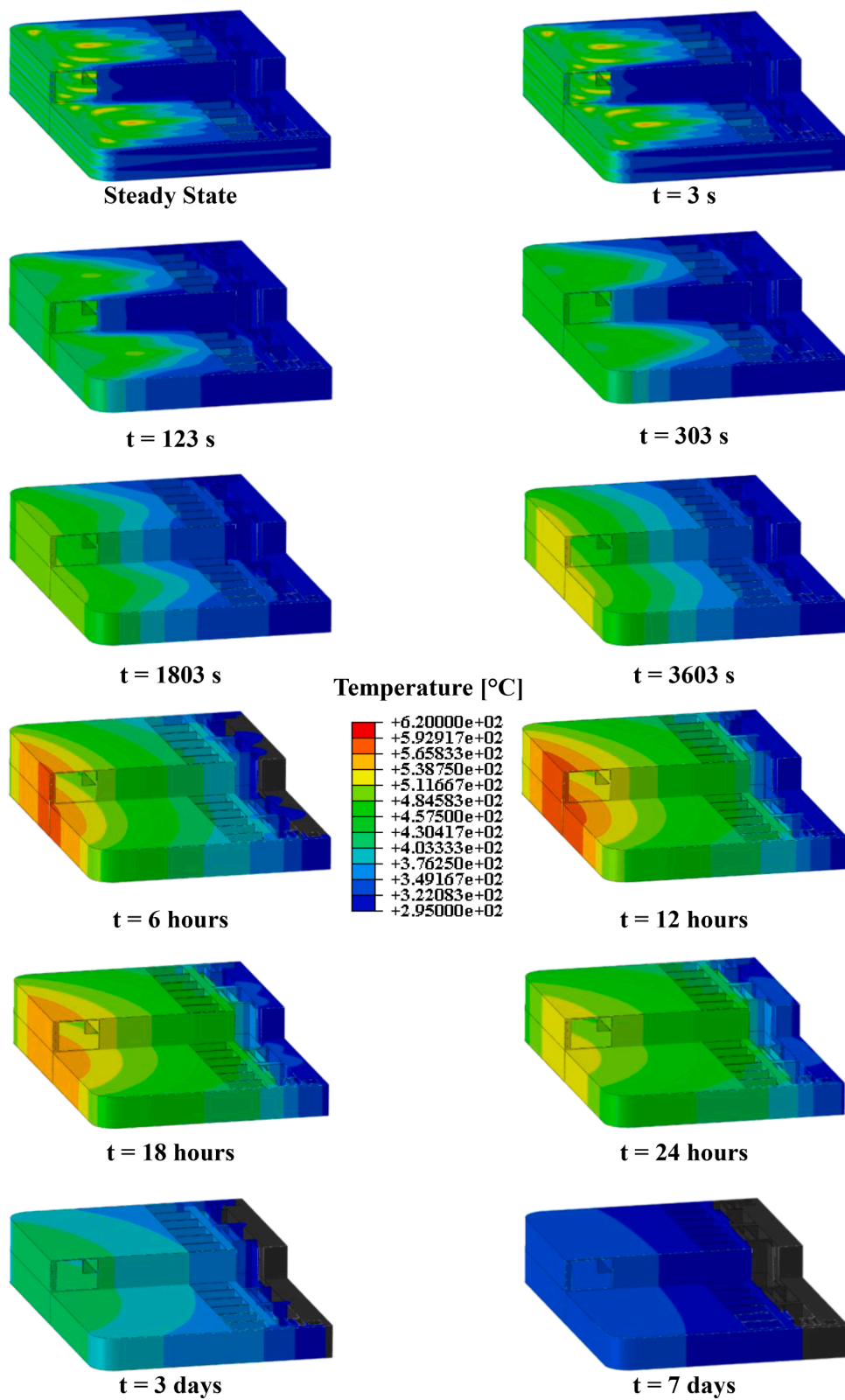


Fig. 15. Eurofer thermal field over the time – Fast plasma termination mode “Case B”.

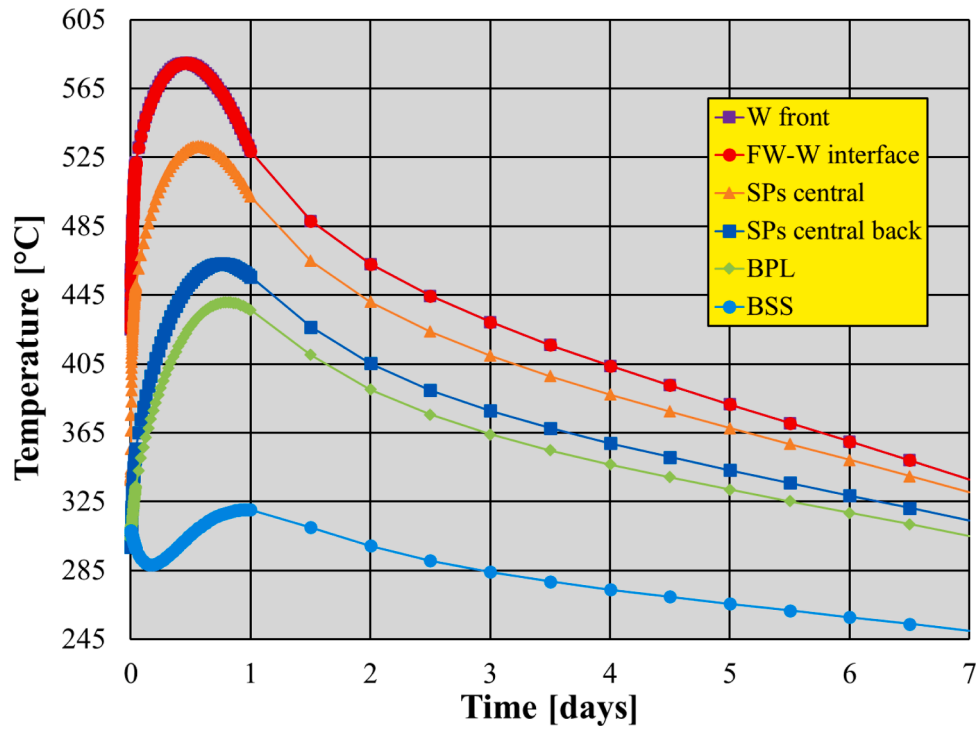


Fig. 16. Eurofer temperature trends at the control nodes - Fast plasma termination mode “Case B”.

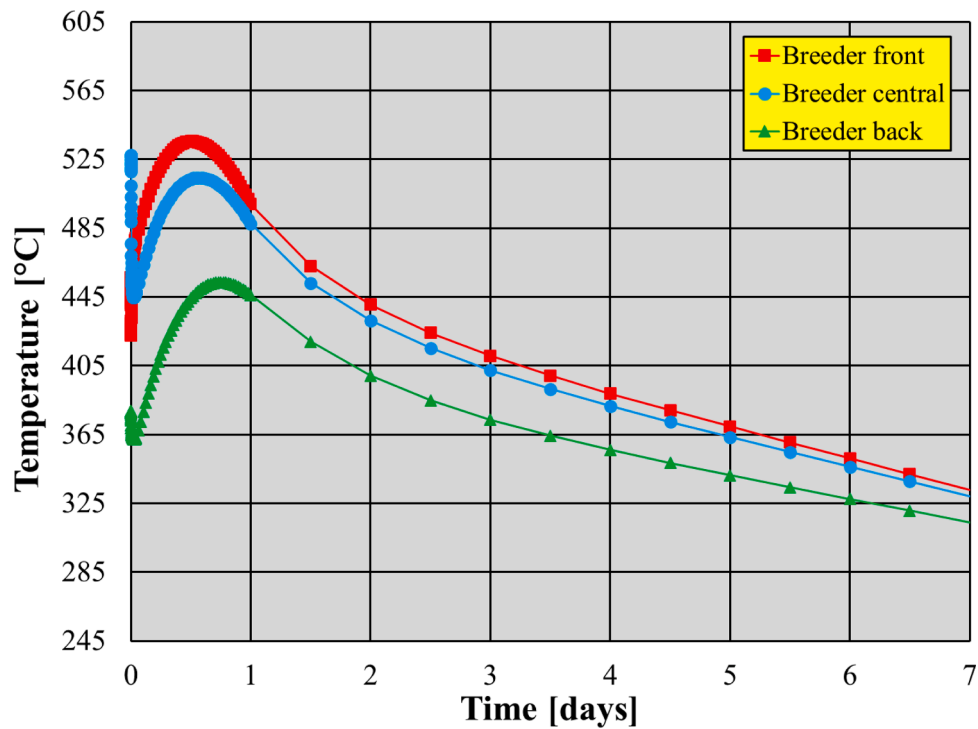


Fig. 17. Breeder temperature trends at the control nodes - Fast plasma termination mode “Case B”.

suggested limit value of 550 °C within FW and breeding zone steel for a long time. Even after 3 days, the temperature within the steel of the FW and the breeding zone is well above the 500 °C. After 7 days, temperatures ranging from ~395 °C to ~435 °C are predicted, suggesting that an auxiliary system should be conceived to help the BB cooling in such a scenario.

Moreover, the temperature trends versus time obtained at the control

nodes for Eurofer and breeder are reported in Figs. 12 and 13. Here, it can be observed that a first peak of ~652 °C is calculated at the FW-W interface control nodes after 88 s, and a second peak of ~648 °C is predicted after ~18.5 h. Also at the other control nodes, temperature grows significantly in the first day after the accident. As to the breeder, the maximum temperature of ~625 °C is achieved after ~19.0 h in the control node “breeder front”.

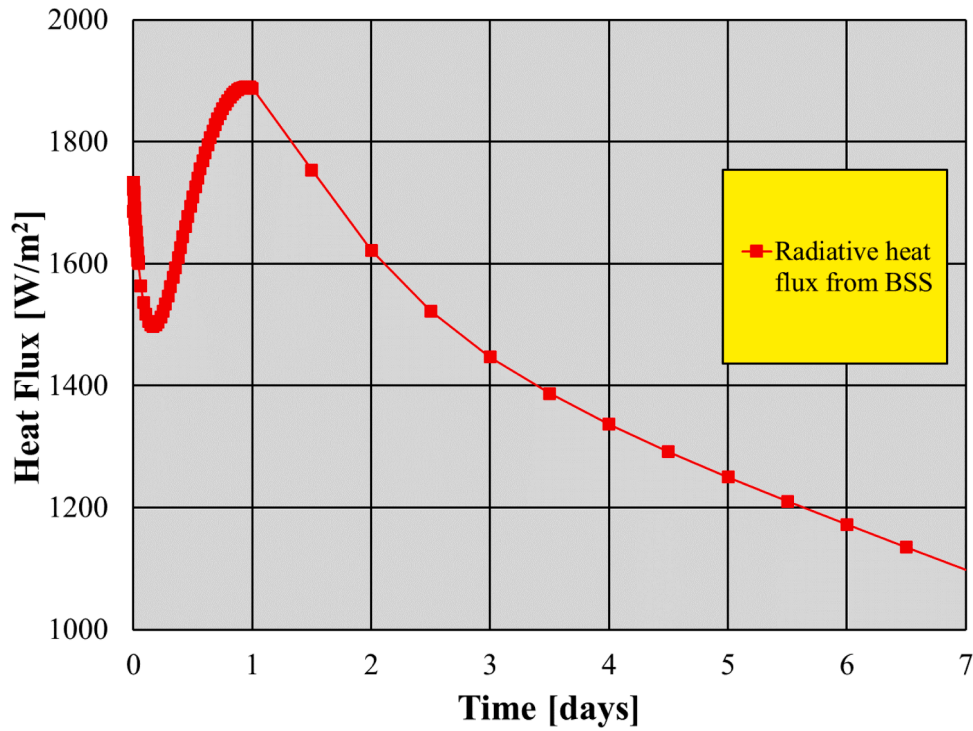


Fig. 18. Heat flux radiated from the BSS - Fast plasma termination mode “Case B”.

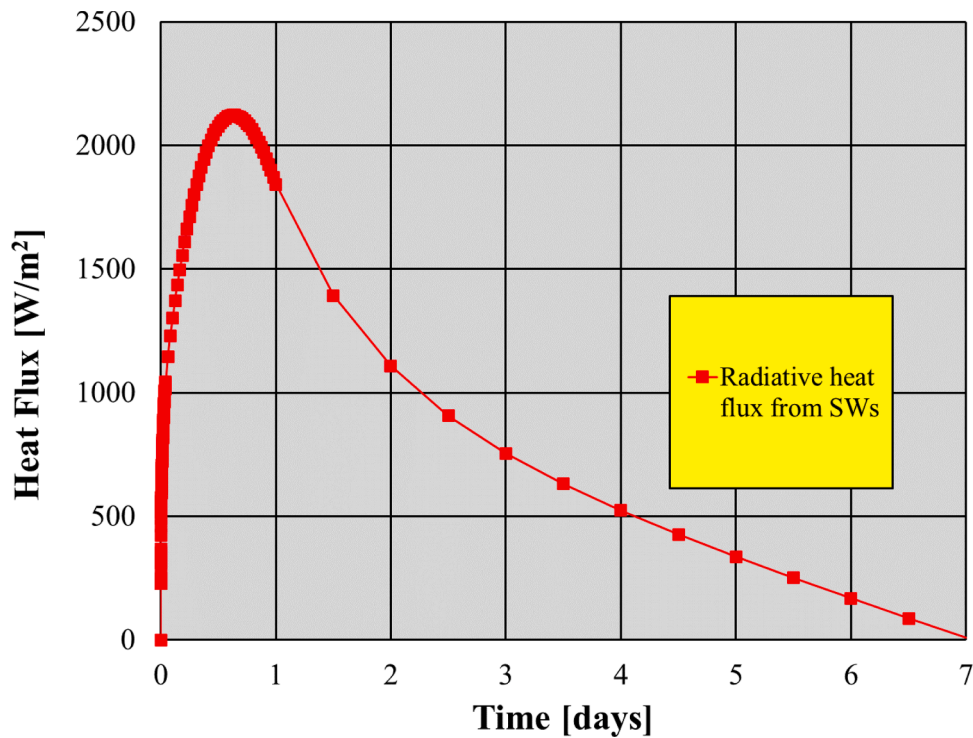


Fig. 19. Heat flux radiated from the SWs - Fast plasma termination mode “Case B”.

In the end, in Fig. 14, the trend of the heat flux radiated from the BSS is shown. As it can be observed, after an initial decrease (the minimum heat flux of  $\sim 1545 \text{ W/m}^2$  is radiated after  $\sim 3.0 \text{ h}$ ) the radiative heat flux power grows up to its maximum value of  $\sim 2850 \text{ W/m}^2$ , achieved after  $\sim 1.5$  days from the accident which is also when the temperature predicted in the BSS control node achieves its maximum value ( $\sim 372.5 \text{ }^\circ\text{C}$ ). Then, the heat flux starts to decrease again. Assuming for the whole BB

system a BSS total surface of  $1650 \text{ m}^2$ , it can be estimated that the thermal power radiated toward the VV ranges from  $\sim 2.55$  to  $\sim 4.70$  MW.

### 5.1.3. Fast plasma termination “Case B”

In this load case, the SWs are allowed radiating towards adjacent segments during the accidental transient since the hypothesis of an

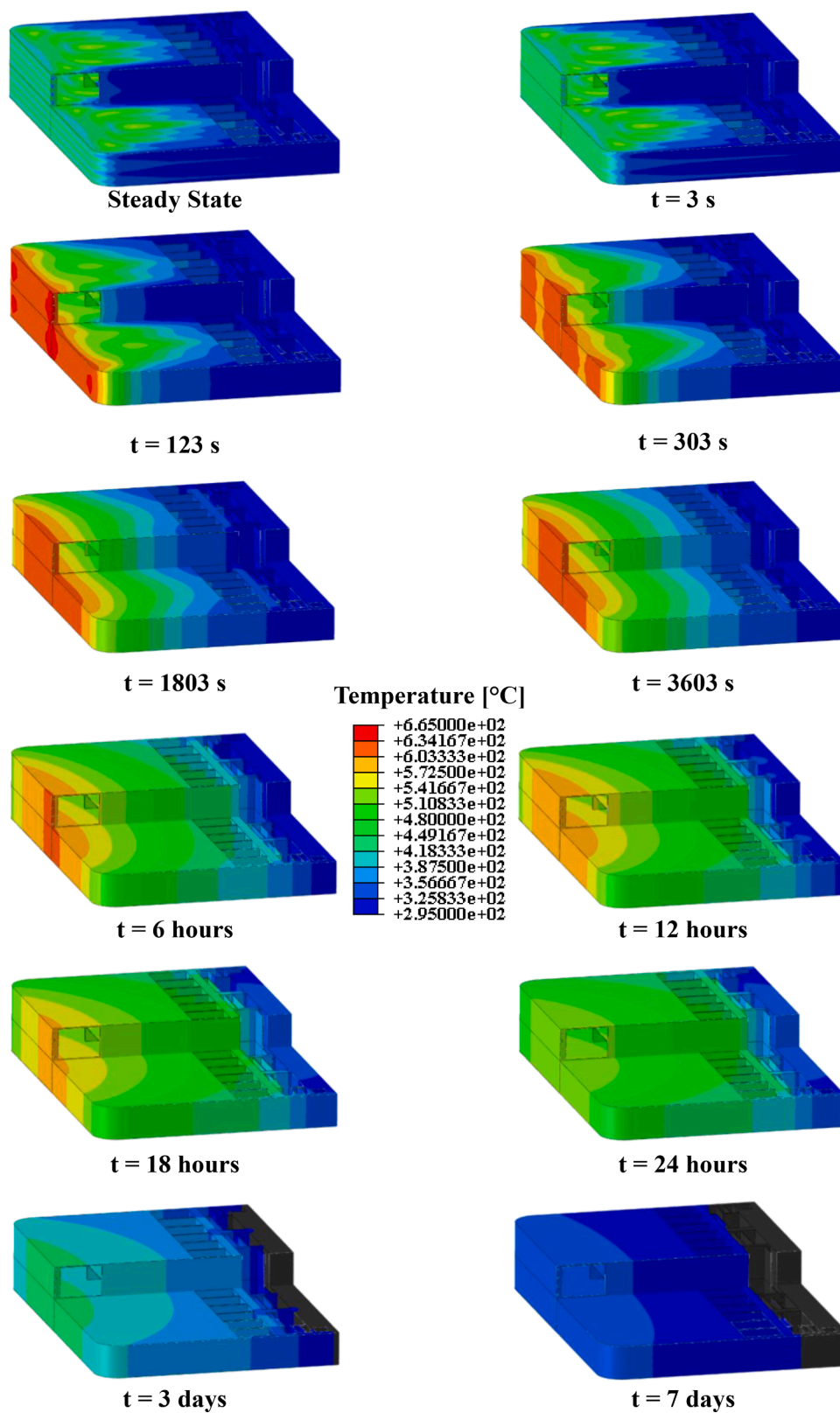


Fig. 20. Eurofer thermal field over the time – Soft plasma termination mode “Case B”.



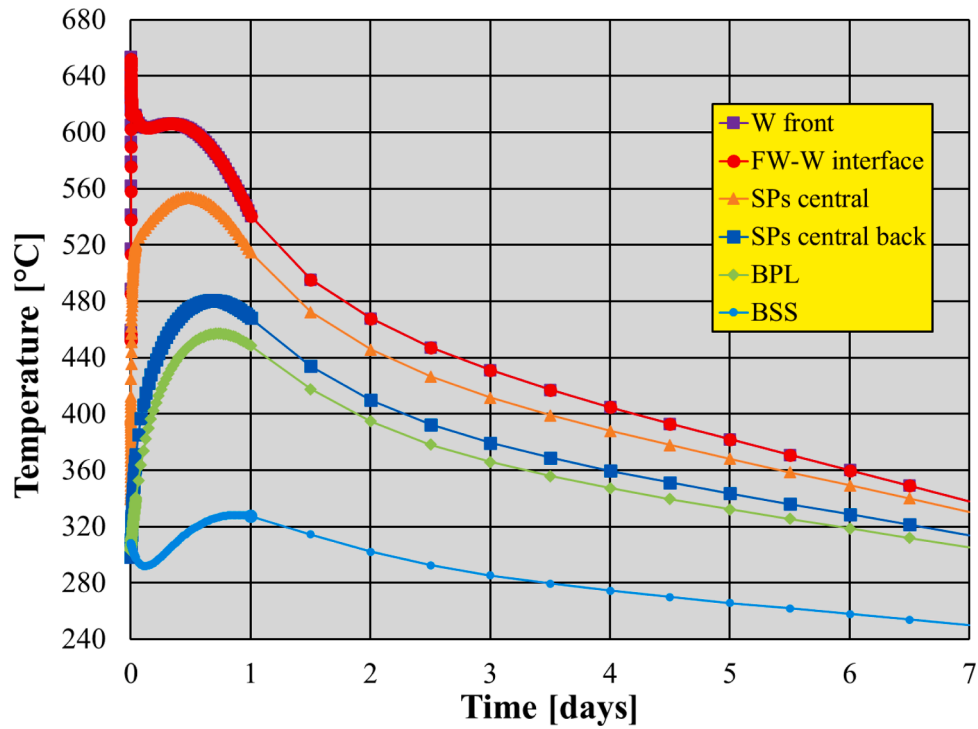


Fig. 21. Eurofer temperature trends at the control nodes - Soft plasma termination mode "Case B".

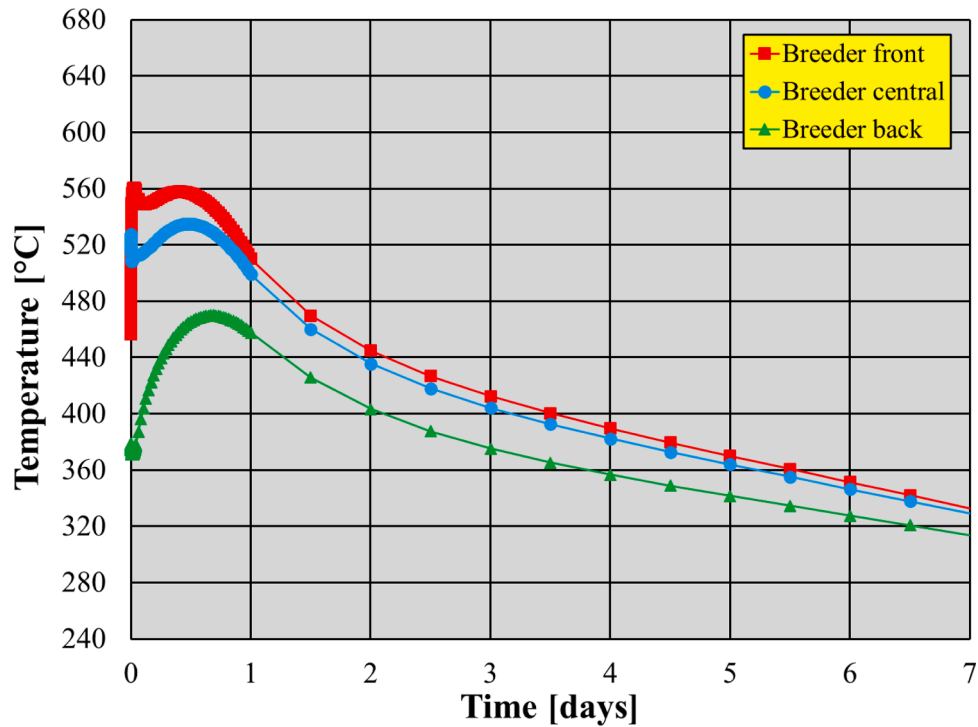


Fig. 22. Breeder temperature trends at the control nodes - Soft plasma termination mode "Case B".

alternate cooling strategy for the BB system is made. The first effect of this assumption is that the predicted thermal fields over the time show a more accentuated toroidal dependence than those obtained from "Case A" analyses. In particular, the Eurofer thermal field over the time is shown in Fig. 15. As it can be observed, even if the plasma is immediately terminated, starting from steady state values the temperatures increase significantly in the first 24 h after the accident occurrence.

Nevertheless, the suggested limit value of 550 °C is slightly overtaken within FW only for some hours whereas it is never reached elsewhere. Hence, giving the SWs the possibility to radiate towards adjacent actively cooled segments seems to be pivotal to reduce the temperature within the BB during the accidental transient. In particular, looking at the Eurofer temperature trend versus time (Fig. 16), at the FW-W interface a maximum temperature of ~ 580 °C is achieved ~11 h after

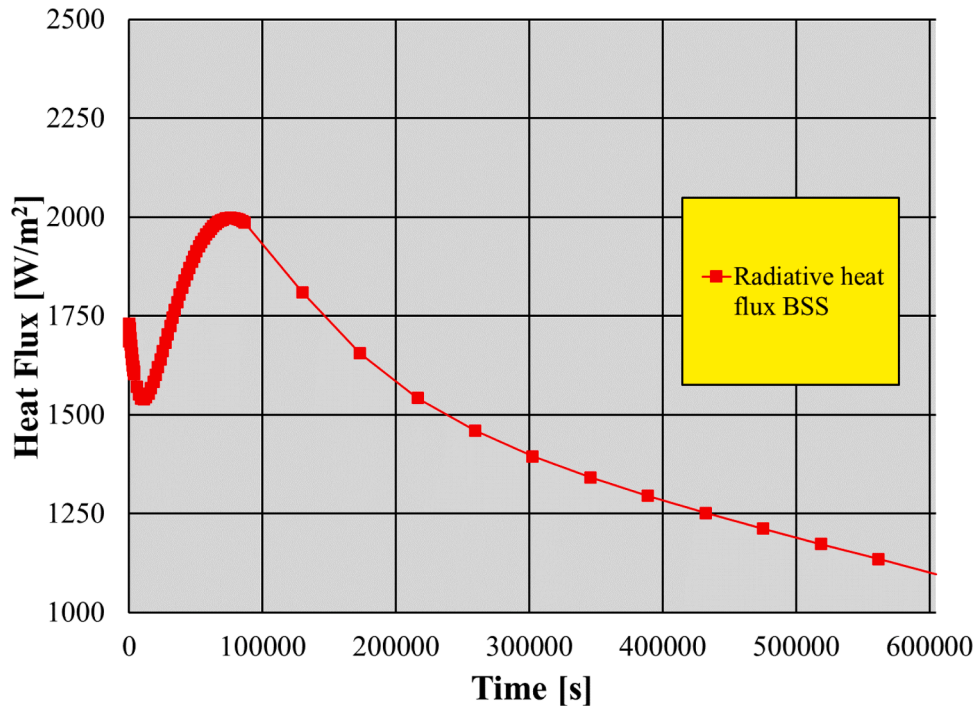


Fig. 23. Heat flux radiated from the BSS - Soft plasma termination mode “Case B”.

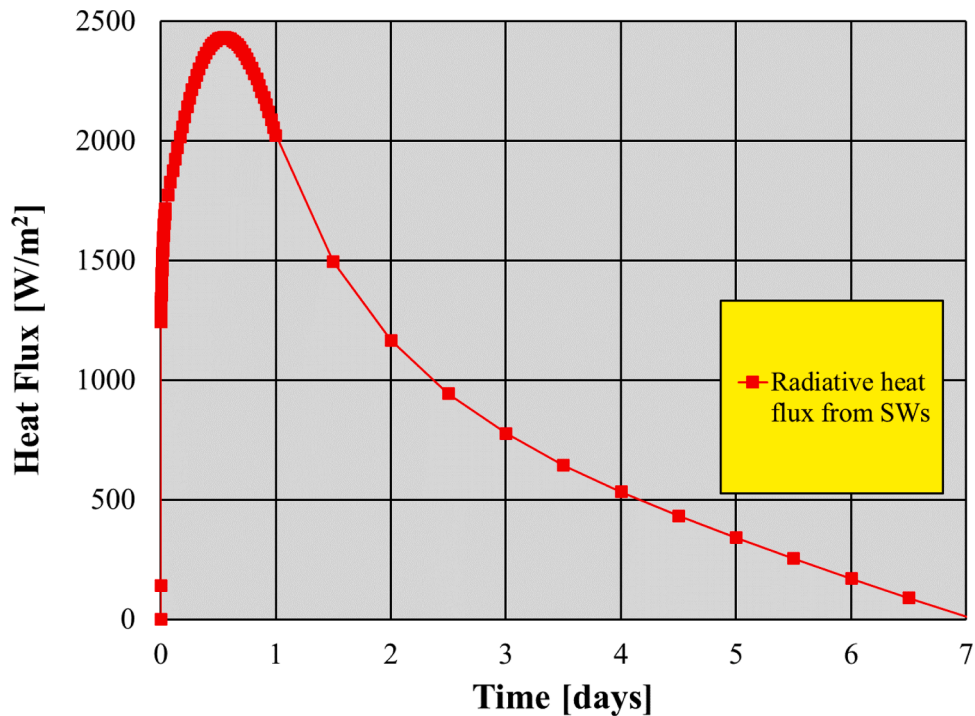


Fig. 24. Heat flux radiated from the SWs - Soft plasma termination mode “Case B”.

the accident. After 7 days, temperatures lower than  $\sim 350\text{ }^{\circ}\text{C}$  are predicted, with the minimum values within the BSS lower than  $295\text{ }^{\circ}\text{C}$  ( $\sim 250\text{ }^{\circ}$  after 7 days).

In the same way, the breeder temperature trends at the control nodes are shown in Fig. 17. Starting from steady state, it can be noted that after 7 days the breeder temperature is widely below  $350\text{ }^{\circ}\text{C}$ , suggesting that local solidifications may occur. In particular, the maximum temperature of  $535.5\text{ }^{\circ}\text{C}$  is achieved after 12 h in the control node “breeder front”.

In addition, in Fig. 18 the trend of the heat flux radiated from the BSS

is reported. As it can be observed, after an initial decrease the heat flux grows up to its maximum value of  $\sim 1890\text{ W/m}^2$ , achieved after  $\sim 22.5\text{ h}$  from the accident which is also when the temperature predicted in the BSS control node achieves its maximum value ( $\sim 320\text{ }^{\circ}\text{C}$ ). It has to be noted that, in this case, the accident occurrence generates the loss of coolant in a half of the BB system. This means that a half of the BSS surface ( $825\text{ m}^2$ ) has been considered radiating with a heat flux equal to the steady state one ( $\sim 1686\text{ W/m}^2$ , since a half of the segments is not affected by the accident remaining in steady state conditions), whereas

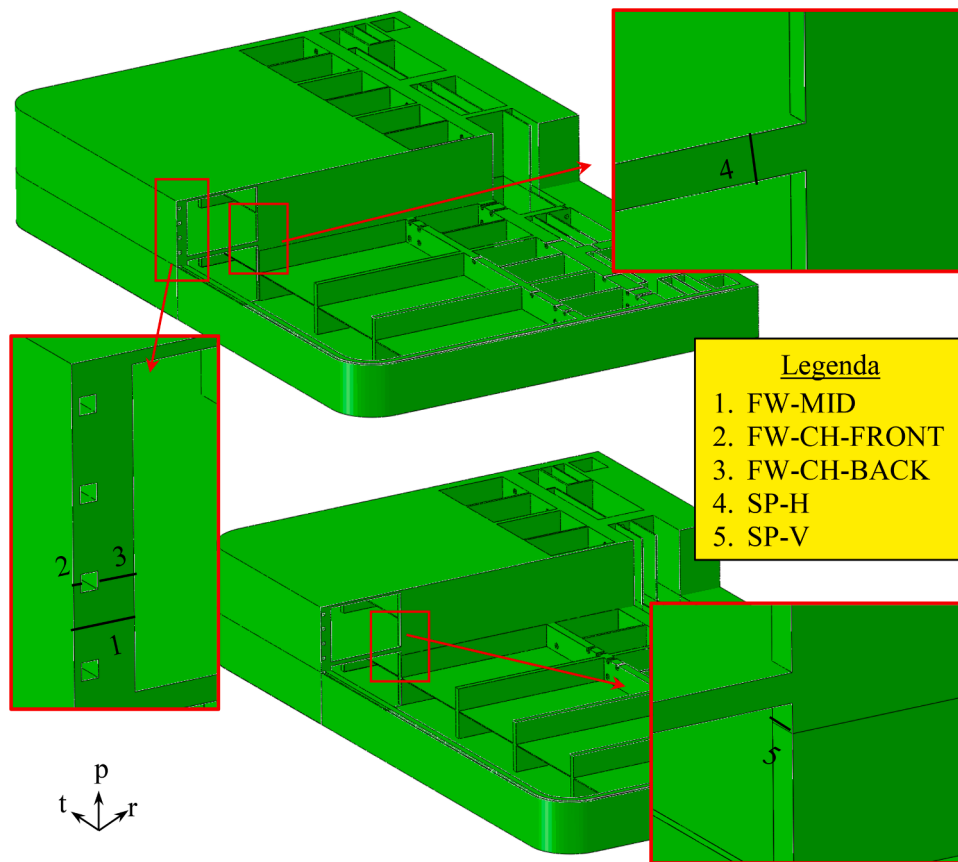


Fig. 25. Paths set-up for the stress linearization procedure.

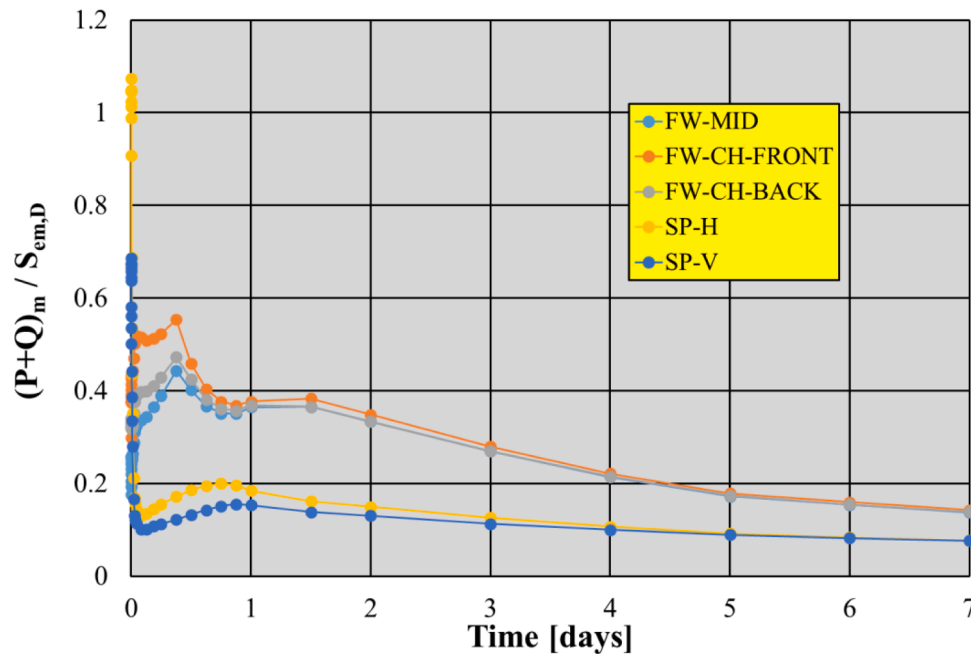


Fig. 26. IPFL criterion - Fast plasma termination mode “Case A”.

the other half is assumed radiating with the time dependant heat flux reported in Fig. 18. This means that, after 22.5 h, the maximum radiative heat power of ~2.95 MW is obtained.

Lastly, the trend of the heat flux radiated from the SWs is reported in Fig. 19. It has to be noted that, in this case, the half of the segments

radiates to the adjacent ones (the latter supposed actively cooled) throughout a SWs total surface of 1188 m<sup>2</sup> (which is the total surface of the half of the segments’ SWs). Hence, also in this case the thermal power radiated by the SWs, removed in any case by the BB cooling system of the half of the segments actively cooled, is estimated

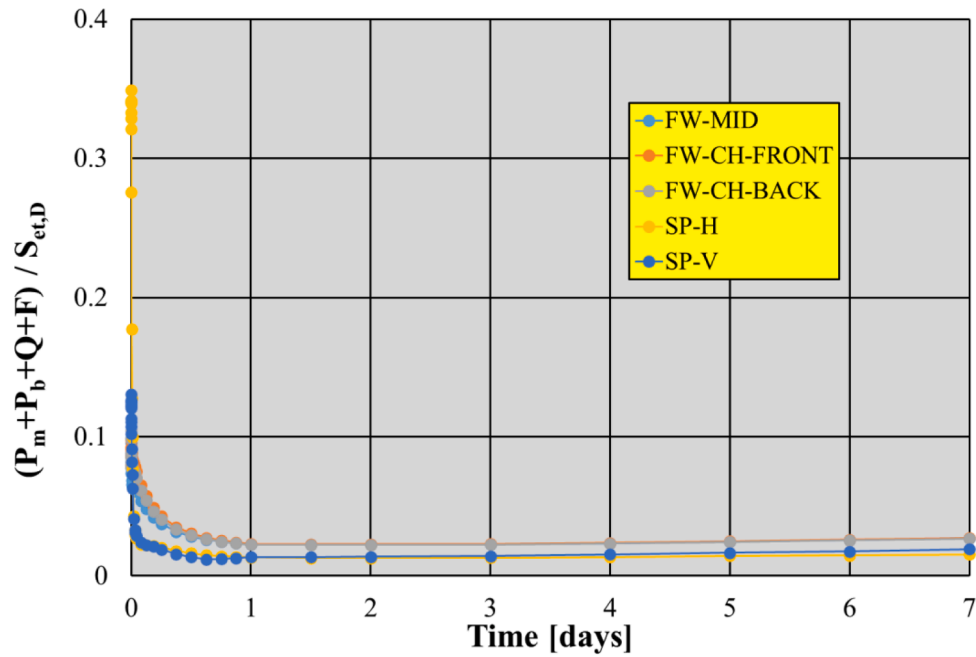


Fig. 27. IF criterion - Fast plasma termination mode “Case A”.

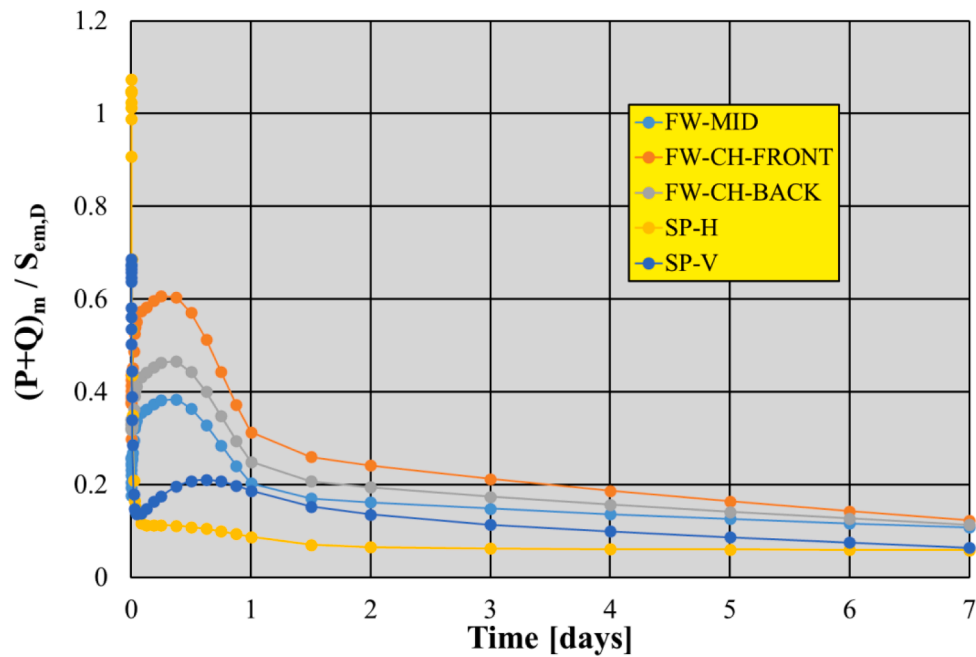


Fig. 28. IPFL criterion - Fast plasma termination mode “Case B”.

multiplying the calculated time-dependant heat flux by the above said total SWs surface. In particular, the heat flux radiated by SWs grows in the first hours after the accident and then decreases. In fact, a maximum value of  $\sim 2100 \text{ W/m}^2$ , corresponding to a maximum radiative power of  $\sim 2.5 \text{ MW}$ , has been calculated after  $\sim 15.5 \text{ h}$ .

5.1.4. Soft plasma termination “Case B”

As to this load case, the Eurofer thermal field over the time is shown in Fig. 20, whereas the temperature vs. time in the Eurofer control nodes are reported in Fig. 21. As it can be observed, even if the plasma is terminated following a ramp-down, the double temperature peak observed within FW in “Case A” is not present here, due to the mitigative effect of the radiating SWs. Starting from steady state values the

temperatures increase significantly in the first 24 h after the accident occurrence exceeding the suggested limit of  $550 \text{ }^\circ\text{C}$  within FW. Nevertheless, the suggested limit value is slightly overtaken within the front part of the SPs only for a few hours whereas it is never reached elsewhere. Hence, giving the SWs the possibility to radiate towards adjacent actively cooled segments seems to be pivotal to globally reduce the temperature within the BB, even in case of soft plasma shutdown. In particular, at the FW-W interface, a maximum temperature of  $\sim 652 \text{ }^\circ\text{C}$  is achieved 88 s after the accident and then the temperature decreases with different slopes. After 7 days, temperatures lower than  $\sim 350 \text{ }^\circ\text{C}$  are predicted, with the minimum values within the BSS lower than  $295 \text{ }^\circ\text{C}$  ( $\sim 250 \text{ }^\circ$  after 7 days).

In the same way, the temperature trends of the breeder control nodes



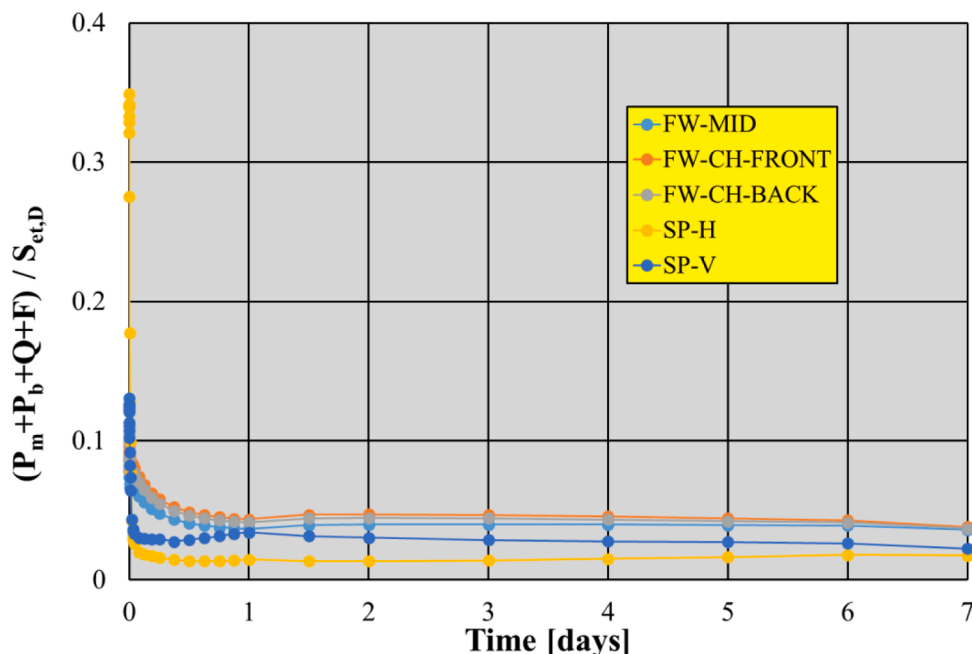


Fig. 29. IF criterion - Fast plasma termination mode “Case B”.

are shown in Fig. 22. Starting from steady state, it can be noted that after 7 days the breeder temperature is widely below  $350\text{ }^{\circ}\text{C}$ , suggesting that local solidifications may occur. In particular, the maximum temperature of  $\sim 560.5\text{ }^{\circ}\text{C}$  is achieved after  $\sim 2200\text{ s}$  in the control node “breeder front”.

In addition, in Fig. 23, the trend of the heat flux radiated from the BSS is showed. As it can be observed, after an initial decrease the heat flux grows up to its maximum value of  $\sim 2000\text{ W/m}^2$ , achieved after  $\sim 21.0\text{ h}$  from the accident which is also when the temperature predicted in the BSS control node achieves its maximum value ( $\sim 328\text{ }^{\circ}\text{C}$ ), then decreases again. Assuming that only the half of the BB segment are faulted whereas the other half is cooled at steady state conditions, this corresponds to a maximum radiative heat power of  $\sim 3.04\text{ MW}$ .

Lastly, the trend of the heat flux radiated from the SWs is reported in Fig. 24. In particular, the heat flux radiated by SWs grows in the first hours after the accident, achieving its maximum of  $\sim 2433\text{ W/m}^2$  after  $\sim 13.0\text{ h}$ , and then decreases. Hence, a corresponding maximum value of  $2.89\text{ MW}$  has been calculated after  $13.0\text{ h}$  for the heat power radiated by the SWs, considering that only the half of the SWs radiates since only the half of the BB segments are not cooled anymore because of the accident.

## 5.2. Thermo-mechanical analysis results

Once obtained the transient thermal response of the WCLL COB segment equatorial region in case of the sudden loss of coolant conditions, the corresponding thermo-mechanical analyses under the four postulated load cases have been carried out. Hence, the fulfilment of the most critical criterion prescribed by the RCC-MRx structural design code, namely the criterion against the immediate plastic flow localization (IPFL), has been verified throughout the transient. Indeed, as emerged from the past campaign of analysis devoted to the design of the WCLL BB [13], such a criterion is the most critical as it encompasses both primary and secondary stress. Moreover, since the IPFL stress limit for Eurofer is thought to be too conservative, the criterion against the Immediate Fracture due to exhaustion of ductility (IF) has been checked as well. Since the postulated load cases refer to a severe accidental condition, the Level D stress limits  $S_{em,D}$  and  $S_{et,D}$  have been taken into account in order to compare, respectively, the obtained primary and secondary membrane stress intensity, indicated as  $(P + Q)_m$ , for what

concerns the IPFL criterion and the total stress intensity, indicated as  $P_m + P_b + Q + F$ , as to the IF criterion. To this goal, a proper set of paths (Fig. 25) has been built and adopted to perform a stress linearization procedure aimed at calculating the stress intensity values.

The obtained results are reported in the following, in terms of the trends versus time of the  $(P + Q)_m / S_{em,D}$  and  $(P_m + P_b + Q + F) / S_{et,D}$  ratios in the different paths and for the four assessed load cases.

Regarding the fast plasma termination mode “Case A” load case, it can be observed (Fig. 26) that, during the transient, in none of the considered paths the IPFL ratio critical value of 1.0 is significantly overtaken. As to the SP-H path for which the criterion is not fulfilled in steady state conditions, the predicted trend shows a quick reduction of the stress level. In particular, for this path, ratio values lower than 1 are predicted from  $\sim 60\text{ s}$  onwards. In the same way, also for the other paths, even if for a certain timespan the trend is increasing, it never reaches the critical value starting to decrease for good from  $\sim 1$  day after the accident onwards. Moreover, looking at the IF criterion verification (Fig. 27), no concerns emerge from the exhaustion of ductility point of view since the ratio between the stress and the limit always remains well below 1.0.

As to the fast plasma termination mode “Case B” load case (Fig. 28), similar considerations can be made. In particular, as to IPFL criterion, it can be observed that the ratios increase in the first day after the accident is more pronounced than in Case A, because of the high thermal gradients originated within the structure as effect of the thermal power radiated by SWs. In any case, the critical value of 1.0 is never achieved. Negligible differences are predicted between Case A and Case B in the first minutes of the transient, since the effect of the SWs irradiations becomes considerable at least after 1 h from the accident. The same conclusion can be achieved looking at the IF criterion (Fig. 29).

As to the soft plasma termination mode “Case A” load case, the plasma ramp-down is the responsible of the non-fulfilment of the IPFL criterion in the first minutes of the transient. Indeed, (Fig. 30) along the paths located within FW an increase of the ratio is predicted, leading to value greater than 0.8 for the FW-MID path and greater than 1.0 for the paths close to the cooling channel. Hence, starting from a good behaviour in steady state, the system seems not to be able to withstand the soft plasma shutdown due to the additional thermal power received during the ramp-down. However, since the IPFL criterion is probably too

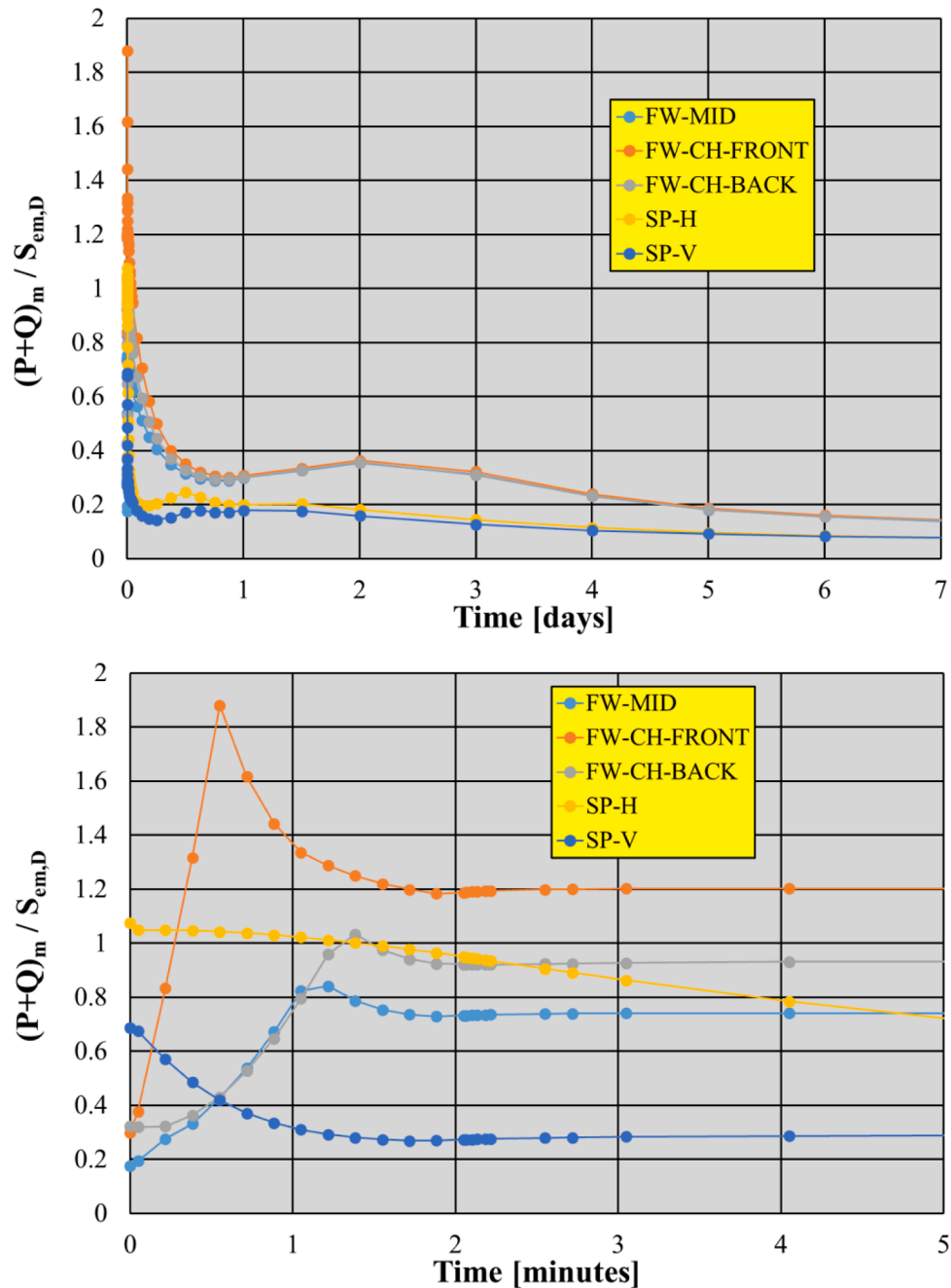


Fig. 30. IPFL criterion - Soft plasma termination mode "Case A".

conservative, the IF criterion has been checked as well showing promising performances against the loss of ductility (Fig. 31).

Analogously, a similar response has been obtained for the soft plasma termination mode "Case B" load case (Figs. 32 and 33). In this case, the effect of the SWs radiation is considerable starting from 1 h after the accident occurrence and, globally, it is the same already observed in the fast plasma termination case. Hence, what happens in the first minutes after the accident is almost identical to what already observed in the previous Case A. Therefore, it can be concluded that the BB alternate cooling scheme does not give any help to safely withstand the soft plasma shutdown.

## 6. Conclusion

In the framework of the EUROfusion consortium research activities,

an exploratory study of the EU-DEMO Water-Cooled Lithium Lead breeding blanket thermal and thermo-mechanical behaviour in case of loss of cooling capability has been performed and here presented.

Four different transient load cases, considering soft/plasma shutdown and uniform/alternate WCLL BB system cooling scheme, have been investigated starting from the nominal steady state conditions. Thermal results have clearly indicated that the predicted temperatures within the Eurofer domain overtake the suggested limit of 550 °C for a long time if the SWs are not allowed radiating (i. e. if a uniform cooling strategy for the BB system is assumed), even in case of fast plasma shutdown. In fact, it has been found that keeping the adjacent segments actively cooled (namely if an alternate BB system cooling strategy is assumed) allows considerably reducing the temperatures within the structural material and, consequently, within the breeder throughout the accidental transient. In any case, since after one week from the

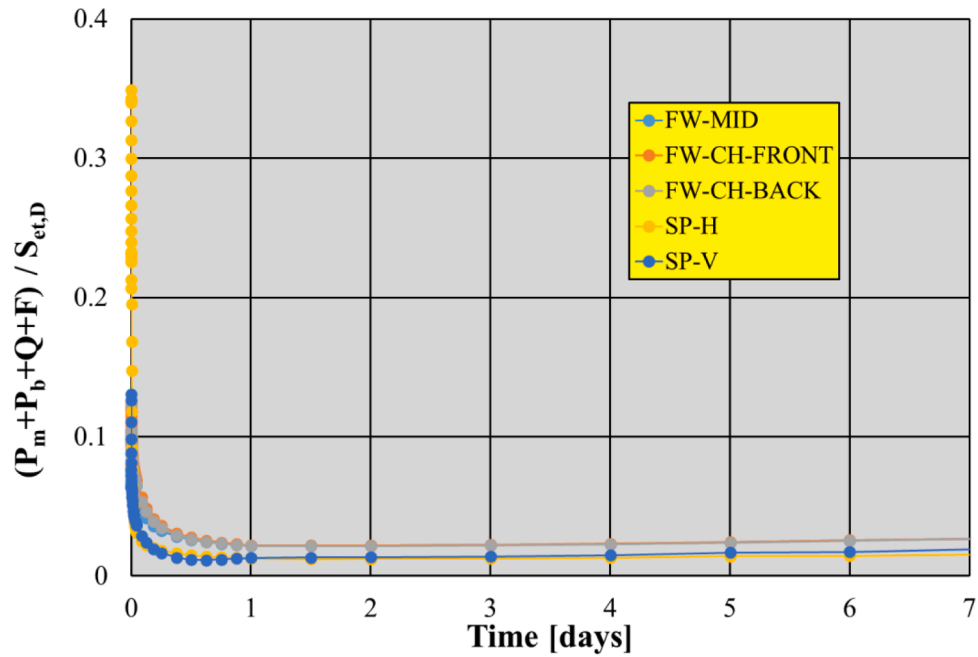


Fig. 31. IF criterion - Soft plasma termination mode “Case A”.

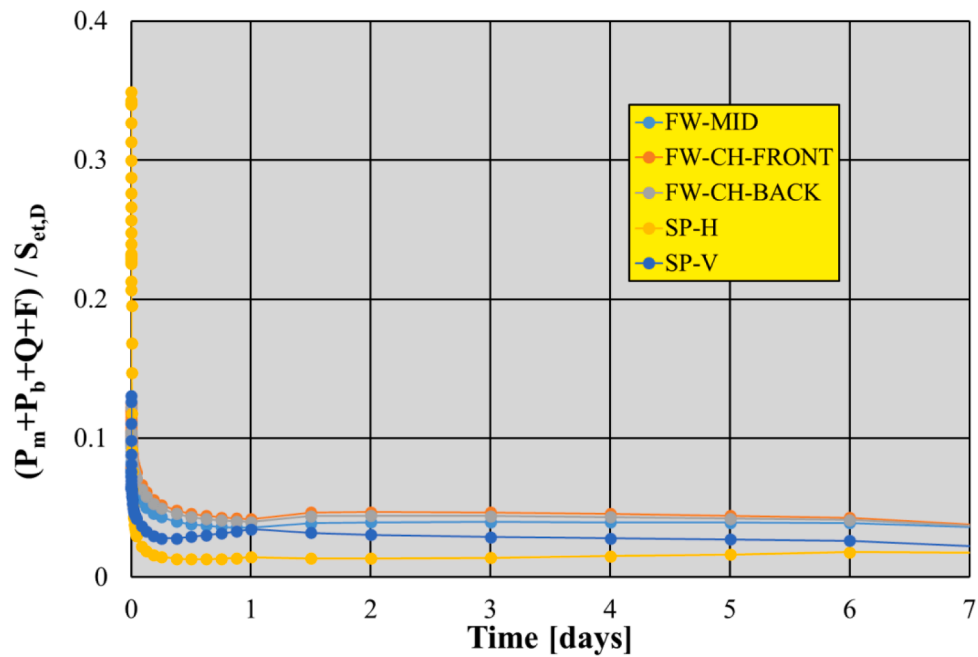


Fig. 32. IF criterion - Soft plasma termination mode “Case B”.

accident occurrence the Eurofer temperature is still well above 250 °C in all the domain, additional cooling systems may be introduced to further reduce the temperature after the accident in sight of the remote maintenance operations. Moreover, the performed study has allowed estimating the time-dependant heat power radiated from the BB system towards the vacuum vessel, in order to give a preliminary input for the design of its cooling system. In the same way, in case of alternate BB system cooling strategy, an estimation of the time-dependant heat power radiated from the SWs of the segments without cooling towards the segments still actively cooled is given in order to provide a preliminary input for the update of the BB cooling system design.

Afterwards, the corresponding transient thermo-mechanical analysis have been carried out with aim of assessing if the WCLL COB segment

equatorial region is able to safely withstand the loads it undergoes during the transient, in view of the RCC-MRx criteria. Results have allowed highlighting that the WCLL BB system, as is, seems not to be able to withstand the soft plasma shutdown, since the plasma ramp-down leads to the non-fulfilment of the considered criterion, whereas a more promising behaviour is predicted under fast plasma termination load cases. Hence, the obtained outcomes suggest making as short as possible the plasma ramp-down and/or improving cooling systems performances to remove the additional power under the postulated accidental conditions. Alternatively, the fast plasma termination (implying a disruption on a limiter) can be considered in case of accident with the aim of not to jeopardise the BB structural integrity.

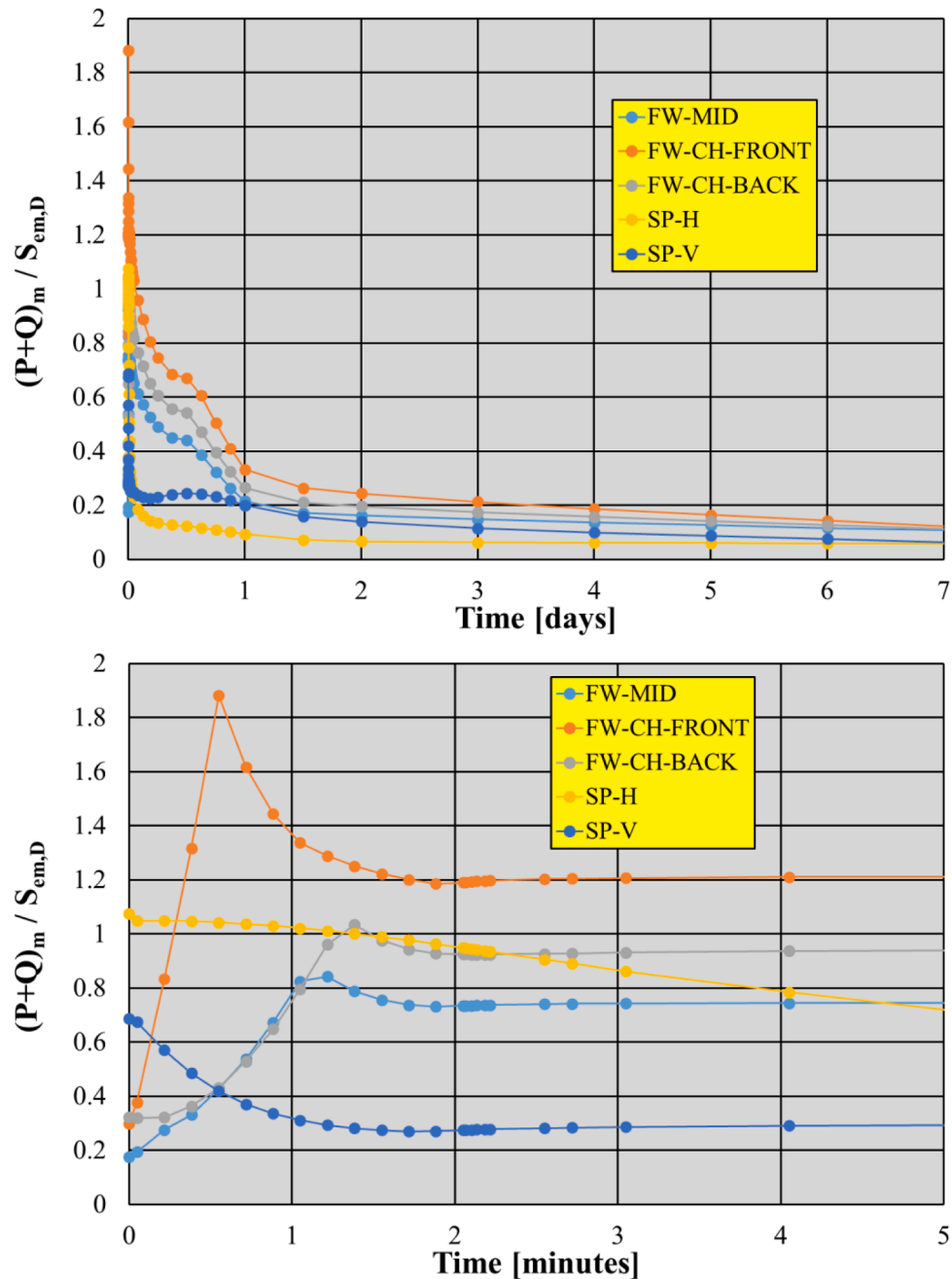


Fig. 33. IPFL criterion - Soft plasma termination mode "Case B".

#### Declaration of Competing Interest

The authors declare that they have no known competing financial interests or personal relationships that could have appeared to influence the work reported in this paper.

#### Acknowledgment

This work has been carried out within the framework of the EUROfusion Consortium, funded by the European Union via the Euratom Research and Training Programme (Grant Agreement No 101052200 — EUROfusion). Views and opinions expressed are however those of the author(s) only and do not necessarily reflect those of the European Union or the European Commission. Neither the European Union nor the European Commission can be held responsible for them.

#### References

- [1] T. Donné et al., European research roadmap to the realisation of fusion energy, EUROfusion, 2018 (ISBN 978-3-00-061152-0).
- [2] RCC-MRx, Design and Construction Rules For Mechanical Components of Nuclear Installations, AFCEN, Courbevoie, France, 2013.
- [3] P. Arena, et al., The DEMO water-cooled lead-lithium breeding blanket: design status at the end of the preconceptual design phase, Appl. Sci. 11 (24) (2021) 11592, <https://doi.org/10.3390/app112411592>.
- [4] E. Gaganidze, Material properties handbook – EUROFER97 (2020), EFDA IDM Ref. EFDA\_D\_2NZHBS.
- [5] D. Martelli, A. Venturini, M. Utili, Literature review of lead-lithium thermophysical properties, Fusion Eng. Des. (138) (2018) 183–195, <https://doi.org/10.1016/j.fusengdes.2018.11.028>.
- [6] E. Gaganidze, F. Schoofs, Material properties handbook – tungsten (2020), EFDA IDM Ref. EFDA\_D\_2P3SPL.
- [7] I. Catanzaro, et al., Development and application of an alternative modelling approach for the thermo-mechanical analysis of a DEMO Water-Cooled Lithium Lead breeding blanket segment, Fus. Eng. Des. 180 (2022), 113195, <https://doi.org/10.1016/j.fusengdes.2022.113195>.

- [8] P. Chiovaro, et al., Assessment of the thermo-mechanical performances of a DEMO water-cooled liquid metal blanket module, *J. Fusion Energy* 34 (2) (2015) 277–292, <https://doi.org/10.1007/s10894-014-9789-z>.
- [9] F. Maviglia, et al., Integrated design strategy for EU-DEMO first wall protection from plasma transients, *Fusion Eng. Des.* 177 (2022), 113067, <https://doi.org/10.1016/j.fusengdes.2022.113067>.
- [10] A. Del Nevo, P. Arena, BB.WCLL-JUS-2-CD1-BB WCLL design description document (DDD), v1.2, 2021, <http://idm.euro-fusion.org/?uid=2NGB4U>.
- [11] T. Berry, T. Eade, (2023) Activation analysis and evaluation of inventories, decay heat, for important components – Activity 2019 – CCFE contribution (Calculation of decay heat in PbLi for entire WCLL reactor), EFDA IDM Ref. EFDA\_D\_2NQL5P.
- [12] G.A. Spagnuolo, et al., Development of load specifications for the design of the breeding blanket system, *Fusion Eng. Des.* 157 (2020), 111657, <https://doi.org/10.1016/j.fusengdes.2020.111657>.
- [13] I. Catanzaro, et al., Analysis of the thermo-mechanical behaviour of the EU DEMO Water-Cooled Lithium Lead central outboard blanket segment under an optimized thermal field, *Appl. Sci.* 12 (3) (2022) 1356, <https://doi.org/10.3390/app12031356>.